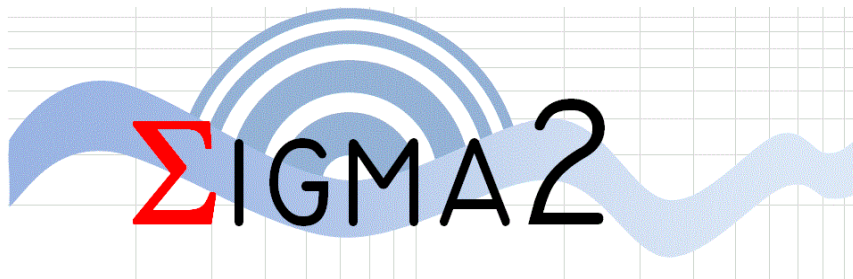





# Develop fragility curves as a function of intensity for full SRA in Intensity domain

Work Package 6 "Ground-motion for engineers"



AUTHORS		REVIEW		APPROVAL	
Name	Date	Name	Date	Name	Date
Marco Fasan	2022/01/16	<i>Y. Bozorgnia</i>  <i>P. Bazzurro</i> 	YYYY/MM/DD	 <b>Public-access</b> <input checked="" type="radio"/> <b>SIGMA-2 restricted</b> <input type="radio"/>	2023/01/13

## Document history

DATE	VERSION	COMMENTS
YYYY/MM/DD	0	

## Executive summary

Seismic Risk Assessment (SRA) depends on uncertainties related both to seismic hazard and structural response of a structure. This two components are usually related to two different disciplines: seismology and structural engineering. For simplicity, a link between this two disciplines is established by selecting a common ground motion intensity measure (IM) to develop hazard and fragility curves. In order to increase confidence in the seismic risk results, a good IM should be able to reduce uncertainties on both sides.

In this deliverable the European Macroseismic Intensity  $I_{EMS}$  is tested as Intensity Measures candidate for use in fragility functions. The broader purpose, not covered in the present study, is to understand if this measure - when used both in hazard and fragility analysis - is capable of reducing the variability in the final seismic risk assessment.

A methodology is proposed to assess  $I_{EMS}$  sufficiency, efficiency and proficiency and results are compared with commonly used IMs. Fragility curves as function of  $I_{EMS}$  are evaluated through Non-Linear Time History Analysis (NLTHA) including the effect of structural collapses.

In comparison with commonly used IMs,  $I_{EMS}$  shows lower efficiency but comparable proficiency (meaning that the dispersion of the fragility functions is similar). Overall,  $I_{EMS}$  seems to be the most sufficient measure among those compared in this study.

## Table of Contents

Document history.....	2
Executive summary .....	2
Table of Contents .....	3
1. Introduction.....	4
2. Reference structure and non-linear time history analysis settings .....	6
3. Intensity Measures selection .....	8
4. Engineering Demand Parameters selection.....	10
5. Performance Levels selection .....	11
6. Record selection.....	12
7. Methodology.....	13
7.1. Fragility development .....	13
7.2. Efficiency and proficiency evaluation .....	15
7.3. Sufficiency .....	16
8. Results and discussion.....	16
8.1. Efficiency and proficiency .....	16
8.2. Sufficiency .....	19
8.3. Regression curves .....	25
8.1. Fragility functions.....	27
8.2. Validity of results.....	29
9. Conclusions and future works .....	32
Bibliography .....	33
APPENDIX 1 Estimated median fragility parameters .....	36
APPENDIX 2 Efficiency and proficiency for the different PLs .....	38
APPENDIX 3 Sufficiency parameters value .....	40

## 1. Introduction

Modern performance-based earthquake engineering (PBEE) approaches have the main goal of predicting the mean annual rate of exceedance  $\lambda$  of some Decision Variable (DV) for specific sites and structures (Cornell and Krawinkler 2000; FEMA 2018). Applying the law of total expectation, this can be expressed mathematically in a simplified form through equation (1).

$$\lambda(DV > dv) = \int P(DV > dv | IM = im) \cdot |d\lambda_{IM}(IM > im)| \quad (1)$$

Where DV is a decision variable (a consequence) and  $d\lambda_{IM}(IM > im)$  is the ground motion hazard curve (or surface) differential for a scalar (or vector) Intensity Measure (IM).

Decision variables can be represented by any measure of interest for the specific risk study such as casualties, monetary losses, business downtime or, in the simplest case, exceedance of some prescribed performance level (PL). In the latter case, assuming that the exceedance of the performance level is associated with the exceedance of a given engineering demand parameter (EDP) threshold, the Seismic Risk Analysis (SRA) reduces to the evaluation of equation (2) (Shome and Cornell 1999).

$$\lambda(EDP > edp_{pl}) = \int P(EDP > edp_{pl} | IM = im) \cdot |d\lambda_{IM}(IM > im)| \quad (2)$$

Where  $edp_{pl}$  represents a given threshold for the specific performance level and  $P(EDP > edp_{pl} | IM = im)$  is the *fragility* of the structure (more correctly this is also called EDP hazard). The fragility is a function that provides the probability of exceeding the PL conditioned to the values of the ground motion intensity measure (IM), i.e. the fragility represents the susceptibility of the structure to seismic damage (Bakalis and Vamvatsikos 2018).

Equation (2) allows to separate two disciplines, namely seismology and structural engineering. Seismologists, applying the Probabilistic Seismic Hazard Analysis (PSHA) (Cornell 1968), provide the intensity measure hazard curve (i.e. the rate of exceedance of each IM value at the site of interest) whereas structural engineers develop the fragility function conditioned on the IM. Note that the IM could also be a vector of different intensity measures and leading to hazard and fragility surfaces (Baker and Cornell 2005; Gehl et al. 2013; Modica and Stafford 2014; Kohrangi et al. 2016c, a, b). Moreover  $\lambda_{IM}$  could also be developed for single or multi earthquake scenarios disregarding their rate of occurrence (i.e. conditioned on the occurrence of a given scenario) (e.g. Fasan 2017; Chieffo et al. 2021).

Therefore, the importance of an appropriate IM selection is clear, as it stands as the unique link between hazard and fragility. In the context of fragility development, an optimal intensity measure should be *efficient*, *sufficient* and *hazard computable* (Luco and Cornell 2007).

Hazard computability means that a Ground Motion Prediction Equation (GMPE) must exist or at least be developable for the selected IM. Moreover, the GMPE also needs to have a relatively small sigma, otherwise its predictability would be impaired and it would not be adequate for hazard computation. An alternative to GMPE could be the use of Physics-Based ground motion simulations (e.g. Paolucci et al. 2018; Hassan et al. 2020).

Fragility is usually evaluated through structural responses estimated via Non-Linear Time History Analysis (NLTHA). There are several procedures to develop fragility functions based on NLTHAs, such as Incremental Dynamic Analysis (IDA) (Vamvatsikos and Cornell 2002), Multiple-Stripe Analysis (MSA) (Bazzurro et al. 1998; Jalayer and Cornell 2009; Baker 2015) and Cloud Analysis (CA) (Luco

and Cornell 2007; Jalayer et al. 2015, 2017). Efficiency means that the IM should predict EDPs accurately, i.e. with low dispersion. Given two IMs, the higher is the efficiency the lower is the number of NLTHAs needed to estimate fragility with the same level of precision.

Given a vector  $\theta_H$  of seismological parameters generally adopted in hazard assessments (i.e. magnitude, distance, soil type, epsilon etc.) a sufficient measure implies that the response of the structure depends only on IM and is independent from  $\theta_H$ :

	$P(EDP > edp_c   IM, \theta_H) = P(EDP > edp_c   IM)$	(3)
--	---	-----

If IM is sufficient, the only information needed from hazard analysis to solve equation (2) is its rate of occurrence and fragility functions can be developed with any record. On the contrary, if IM is insufficient further information about  $\theta_H$  is needed for an accurate and consistent record selection in order to develop unbiased fragility functions. Therefore, since generally there is no sufficient IM, a key aspect is also ground motion selection.

Other characteristics of an optimal IM referred to in the literature are *practicality*, i.e. the level of dependence of the structural demand on the level of IM (evaluated as the value of the slope of the EDP | IM relationship coming from cloud analysis), and *proficiency*, which is the combination of efficiency and practicality (Padgett et al. 2008).

In the context of Seismic Risk Analysis, equation (2) should consider both uncertainties in hazard and fragility analysis. Therefore, to reduce the final overall variability of  $\lambda(EDP > edp_{pl})$  an optimal intensity measure should also present a low variability given  $\theta_H$ , i.e. a low standard deviation  $\sigma_{lnIM}$  of the GMPE and a low dispersion of  $\lambda_{IM}$  (that comes from the inclusion of aleatory and epistemic uncertainties in hazard analysis).

It is then clear that the selection on an IM that reduces the overall variability of  $\lambda(EDP > edp_{pl})$  is not straightforward as this variability is a combination of hazard and fragility uncertainties and inherent variability. This deliverable presents the evaluation of the European Macroseismic Intensity  $I_{EMS}$  as a candidate intensity measure for the development of fragility functions. The broader purpose, not covered in the present study, is to understand if this measure - when used both in hazard and fragility analysis - is capable of reducing the variability in the final seismic risk assessment.

Seismic Hazard Assessment (either probabilistic or deterministic) can be done also using macroseismic intensity as intensity measure taking advantage of the longer duration of historical catalogues compared with instrumental ones. Macroseismic intensity represents a measure of the strength of the ground shaking inferred from the mean damage observed in a homogeneous area and it is the only hazard intensity measure that describes the physical effects of earthquakes on buildings (Klügel and Stäuble-Akçay 2018). Hence,  $I_{EMS}$  should be strictly correlated with the damaging potential of a signal. In particular, the European Macroseismic Scale - EMS (Grünthal 1998) should lead to consistent measures of the strength of the signal even if the built environment where the macroseismic intensity is assessed is very different. This should be assured by the procedure described in the EMS documentation. This procedure mainly consists in:

- Differentiation of structures into vulnerability classes (A-F);
- Classification of damage grade (1-5);
- Definition of the quantity (few-many-most) of buildings falling into each class that have suffered a certain damage grade;
- Definitions of intensity degrees (I-XII).

Clearly, each step performed in the assignment of intensity introduces new uncertainties on the real intensity value. Uncertainties are mainly related to the subjectivity on the field definition of (Musson et al. 2010):

- vulnerability class of the building;
- damage grade reached by the building.

Since few accelerograms are recorded directly inside areas where the macroseismic intensity is also evaluated, the possibility to assign the intensity to other recorded or simulated accelerograms can help to perform damage consistent risk assessments, increasing the number of available accelerograms to be used. This issue is particularly important if the fragility analysis aims to evaluate the effects of collapses, since there are few recorded accelerograms capable of inducing collapse in modern code-conforming seismic designed buildings. As first part of this study, a methodology to assign  $I_{EMS}$  to accelerograms was proposed using regression analysis on available data extracted from a database of real signals built specifically for this purpose. The proposed methodology tries to simulate numerically the assignment procedure of macroseismic intensities on field and is based on regression equations between intensity and linear or non-linear ground motion parameters. Non-linear parameters are extracted from non-linear time history analysis using non-linear SDOF systems representative of the non-linear behaviour of different buildings vulnerability classes. Details of this analysis are reported in the first deliverable of this task (Fasan 2020).

In order to increase the number of available accelerograms, a second deliverable focused on the construction of a database of Physics-Based simulated ground motions. Details on the development of this database can be found in Fasan and Barnaba (2021).

In this deliverable a procedure based on Modified Cloud Analysis (Jalayer et al. 2017) is used to develop fragility functions for a reference structure based on  $I_{EMS}$  and including effects of collapses. Cloud Analysis is used since it is based on the use of unscaled records avoiding possible biases introduced by scaling (Luco and Bazzurro 2007; Zacharenaki et al. 2014). A comparison of  $I_{EMS}$  efficiency, proficiency and sufficiency with other commonly used IMs is presented. To assess the measure up to collapse, records were selected from the above-mentioned database of synthetic signals. At the end validity of results is checked against real signals.

The EMS scale is chosen since it is the reference macroseismic scale in Europe since 1998 and its vulnerability model is the most complete and updated. Nevertheless, the same procedure proposed here can be applied with any macroseismic scale.

The methodology is developed and proposed in the framework of the European project Seismic Ground Motion Assessment 2 (SIGMA-2, <http://www.sigma-2.net/>).

## 2. Reference structure and non-linear time history analysis settings

The reference structure adopted is a five-storey reinforced concrete frame. It is characterized by a square plan of 15m width subdivided in 3 bays with 5m length each. The height of each storey is 3m, for a total height of 15m (Figure 1). Gravitation permanent loads consist in permanent structural loads due to self weight of structural elements, 3.1 kN/m<sup>2</sup> for the floor structural system (reinforced concrete slab), 1.3 kN/m<sup>2</sup> for the flooring and 2 kN/m<sup>2</sup> for internal partition walls. At each floor a live load of 2 kN/m<sup>2</sup> is considered. The roof floor is designed with a snow live load of 0.8 kN/m<sup>2</sup> and no partitions. The seismic action is defined according to the Italian Building Code (C.S.LL.PP 2018) for a moderate hazard site. The parameters defining the Uniform Hazard Spectrum, amplified due to a soil C type are: ground acceleration  $a_g = 0.27$ , ground acceleration spectral amplification  $F_0 = 2.48$  ( $a_g \times F_0$  gives the spectral acceleration plateau value), and corner period  $T_c = 0.33s$  (i.e. the period at the end of the section with constant spectral acceleration).

Using a response spectrum analysis to obtain the maximum stress values, beams and columns are designed according to the Italian Building Code (NTC18 [5]) considering a low ductility class (Class B) and adopting a behaviour factor of 3.9. The weak beam/strong column capacity design criteria is applied and shear forces in members are evaluated from the flexural capacity of their critical regions, thus preventing any shear weak failure. Floors are considered as rigid diaphragms and a fixed support is applied at the base nodes. A strength class C28/35 was adopted for concrete, while B450C was adopted for steel as defined by the Italian Building Code.

The first three vibrational modes of the designed structure are shown in Figure 2 whereas vibrational properties and mass participation ratios (MPR) for the first nine modes are described in Table 1. The fundamental translational modes have mass participation higher than 80%.

Vibrational modes are completely decoupled since there is no eccentricity between the centre of mass and the centre of stiffness. Due to the lower height of the beams of the outer frames with respect to the other ones, the greater translational stiffnesses are concentrated in the vicinity of the centre of gravity making the second mode rotational and not translational (but still regular since there is no mass in the other directions).

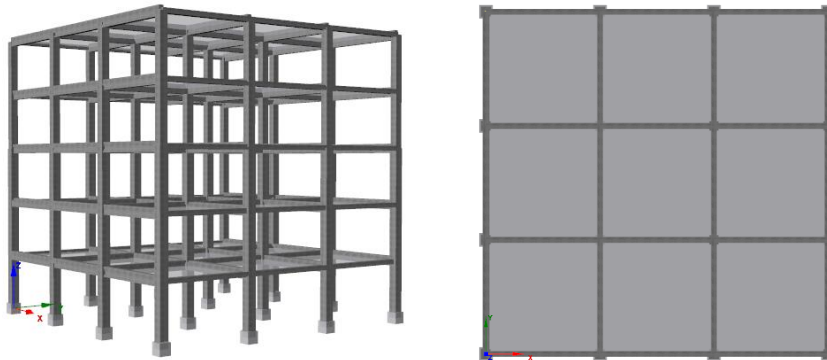


Figure 1: Analysed RC frame: perspective (left) and plan view (right)

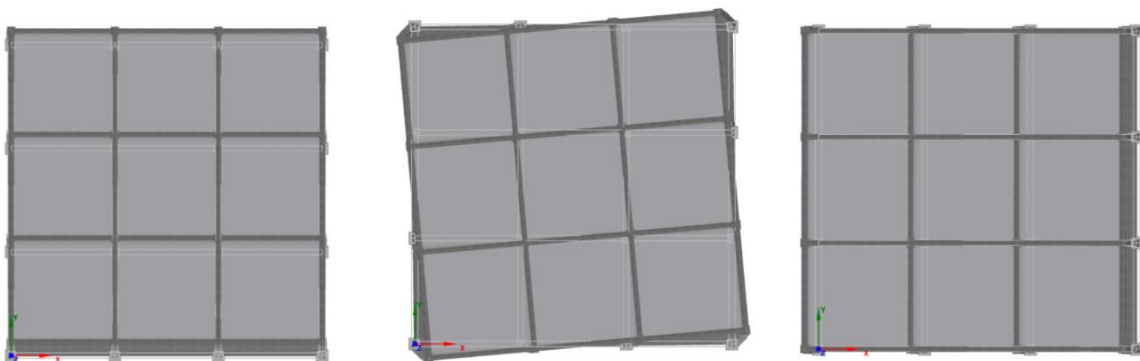


Figure 2: 1<sup>st</sup>, 2<sup>nd</sup> and 3<sup>rd</sup> vibrational model of the considered frame

**Table 1: Periods (T) and mass participation ratios (MPR) for the translational (X and Y) and rotational (RZ) degree of freedom**

Mode n°	T (s)	MPRX (%)	MPRY (%)	MPRRZ (%)
1	0.96	0.00	0.80	0.00
2	0.85	0.00	0.00	0.81
3	0.75	0.82	0.00	0.00
4	0.29	0.00	0.12	0.00
5	0.26	0.00	0.00	0.11
6	0.24	0.11	0.00	0.00
7	0.15	0.00	0.05	0.00
8	0.14	0.00	0.00	0.05
9	0.13	0.04	0.00	0.00

Non linear time history analysis (NLTHAs) are performed using the software Seismostruct (Seismosoft 2021). Both material and geometrical non-linearities are included.

Material non-linearities in beams and columns are accounted for using a force-based inelastic frame element (*infrmFB*) that adopts a diffused plasticity model via the use of fiber-section discretization. A total number of 5 integration sections with 150 discretized fibers is used for each beam element. As regard the concrete material, two constitutive laws are used according to the Mander model (Mander et al. 1988). An unconfined model is used for the cover, characterized by a peak compressive strength  $f_c = 28 \text{ N/mm}^2$  at a strain  $\varepsilon_{c0} = 0.2\%$  and an ultimate strain  $\varepsilon_{cu} = 0.35\%$ . A confined model is used for the core and is characterized by a peak strength that varies as a function of the stirrups confinement (around 1.3 to 1.4 the unconfined peak strength) and an ultimate strain value  $\varepsilon_{cu} = 0.8\%$ . The reinforcement is modelled with the Menegotto-Pinto constitutive law adopting a mean yield strength  $f_y = 450 \text{ N/mm}^2$  (lower bound  $390 \text{ N/mm}^2$ ) and a strain hardening parameter of 0.5%. An elastic modulus of  $32000 \text{ N/mm}^2$  and  $210000 \text{ N/mm}^2$  is adopted for concrete and reinforcing steel respectively.

A Rayleigh damping is used, for which it is necessary to define two vibrational periods and a target damping factor for each of the two chosen modes. The two periods are chosen in order to avoid over damping of higher modes and elongated modes due to plastic deformations and consist in 1.5 times the first vibrational period (1.425s) and the period that leads to a cumulative mass participation ratio of 90% (0.241s). The target damping factor is 3% (ASCE 2014). The Hilber - Hughes – Taylor integration scheme is used.

### 3. Intensity Measures selection

In this study the focus is placed on scalar intensity measures. For comparison with  $I_{EMS}$ , the selected ones are among the most referred to in practice and literature. The first two IMs selected are structure independent as it is  $I_{EMS}$  (i.e. they do not depend on vibrational properties of the structure). They are the Peak Ground motion Acceleration (PGA) and the Cumulative Absolute Velocity (Reed and Kassawara 1990).

$CAV = \int  a_g(t)  dt$	(4)
--------------------------	-----



One of the most used IMs is the spectral acceleration at first mode  $S_a(T_1)$ . As the reference structure and NLTHAs are 3D, the IM should account for the main vibrational properties in both directions. Hence, here spectral acceleration is evaluate at a mean period  $T_{1m}$  evaluated as the average of the values of the fundamental periods in each direction (FEMA 2018).

$$S_a(T_{1m}) = S_a\left(\frac{T_{1x} + T_{1y}}{2}\right) \quad (5)$$

The fourth intensity measure is the average spectral acceleration defined as the geometric mean of the spectral accelerations over a range of periods (Eads et al. 2015; Kohrangi et al. 2016a).

$$S_{a,avg}(T_i) = \left[ \prod_{i=1}^n S_a(T_i) \right]^{1/n} \quad (6)$$

This measure is used as it has been proven efficient, therefore its performance can be a good comparison metric (Ebrahimian et al. 2015; Kazantzi and Vamvatsikos 2015; Kohrangi et al. 2016c). The range of periods should be selected in order to include higher modes effects and period elongations due to accumulation of damage. Here five periods are selected, including modes with mass participation higher than 10%.

$$T_i = [T_{2m}, \min[(T_{2m} + T_{1m})/2, 1.5T_{2m}], T_{1m}, 1.5T_{1m}, 2T_{1m}] \quad (7)$$

Where  $T_{2m}$  is mean of the periods of the second mode in the two orthogonal directions.

According to Fasan (2020), an “instrumental” macroseismic intensity  $I_{EMS}$  can be assigned to any signal based on the following relation:

$$I_{EMS} = e^{\left(\ln(6.012) + 0.133 \cdot \ln(\mu_{kin,avg}) + \epsilon \cdot \sigma_{\ln(I_{EMS})}\right)} \quad (8)$$

Where  $\mu_{kin,avg}$  represents the average kinematic ductility reached by 141 different non-linear SDOF systems representing different buildings and vulnerability classes:

$$\mu_{kin,avg} = \frac{\sum_{i=1}^N \frac{\delta_{max,i}}{\delta_{y,i}}}{N} \quad (9)$$

$N = 141$  represents the number of SDOF systems used to describe the EMS building typologies.

$\delta_{max,i}$  is the maximum displacement reached by SDOF  $i$

$\delta_{min,i}$  is the minimum displacement reached by SDOF  $i$

$\delta_{y,i}$  is the yielding displacement of SDOF  $i$

$F_{y,i}$  is the yielding force of SDOF  $i$

The parameter  $\sigma_{\ln(I_{EMS})} = 0.140$  is the standard deviation of the logarithm of  $I_{EMS}$ , whereas  $\epsilon$  is a random normal variable with zero mean and unitary standard deviation. Equation (8) is used to assign  $I_{EMS}$  to the selected simulated records. The inclusion of the term  $\epsilon \cdot \sigma_{\ln(I_{EMS})}$  allows to account for observed variability around the mean. It must be emphasized that this is a method that attempts to instrumentally assign the macroseismic intensity to a signal. This measure, like PGA and CAV, must be seen as a characteristic of the signal and therefore independent of the building to which the signal is applied.

The last IM considered is the expected macroseismic intensity  $I_{EMS,avg}$  given  $\mu_{kin,avg}$ , defined as

$$I_{EMS,avg} = \sum_{i=1}^{12} I_i \cdot P[I = i|IM] \quad (10)$$

Where  $P[I = i|IM]$  is the probability of experiencing exactly the macroseismic intensity  $I_i$  given the occurrence of  $\mu_{kin,avg}$ .

Summarizing, the following six IMs are used:

- PGA;
- CAV;
- $S_a(T_{1m})$ ;
- $S_{a,avg}(T_i)$ ;
- $I_{EMS}$ ;
- $I_{EMS,avg}$ ;

Apart from  $I_{EMS}$  and  $I_{EMS,avg}$ , the listed IMs can be calculated for different representations of motion, thus assuming different values depending on the selected ground motion component. Since the NLTHAs are 3D, ground motion should be represented by a bidirectional component. Moreover, the motion component itself may have an influence on the efficiency or sufficiency of an IM. Therefore, the following bidirectional representations of motion components are considered in this study:

- The geometric mean of the as recorded signals ( $GM$ );
- The median geometric mean value over all possible non redundant rotation angles ( $GM_{RotD50}$ );
- The maximum geometric mean value over all possible non redundant rotation angles ( $GM_{RotD100}$ ) (Boore et al. 2006);
- The mean value over all possible non redundant rotation angles ( $RotD50$ )(Boore 2010);
- The maximum mean values over all possible non redundant rotation angles ( $RotD100$ ).

This leads to a total of 22 investigated intensity measures.

Apart from  $I_{EMS}$  and  $I_{EMS,avg}$ , the selection of intensity measures was based solely on the choice of the most commonly used measures for the development of fragility functions in the past (e.g. pga), the most used currently (e.g.  $S_a$ ) and the most promising according to latest research (e.g.  $S_{a,avg}$ ).

#### 4. Engineering Demand Parameters selection

Generally, structural and non-structural damage of deformation-sensitive components is correlated with the interstorey drift occurring at each floor. The Interstorey drift time history at floor  $i$  in direction  $j$  is defined as:

$$IDR_{i,j}(t) = \frac{\delta_{i,j}(t) - \delta_{i-1,j}(t)}{h_i} \quad (11)$$

Where  $\delta_{i,j}(t)$  is the displacement at floor  $i$  in direction  $j$  at time  $t$  and  $h_i$  is the interstorey height.

To use a unique directionless value, the maximum (resultant) interstorey drift at storey  $i$ , is taken as the peak (in time) of the SRSS of the IDR in the two main orthogonal directions:

$$MIDR_i = \max \left( \sqrt{IDR_{i,x}^2(t) + IDR_{i,y}^2(t)} \right) \quad (12)$$

Finally, the maximum interstorey drift observed in the building is adopted as a single EDP to define the level of damage reached in the structure:

$$MIDR = \max(MIDR_1, \dots, MIDR_n) \quad (13)$$

Where  $n$  is the number of storeys.

MIDR is able to relate the maximum rotations reached at the component level with the global deformations (Jalayer and Cornell 2009; Jalayer et al. 2015).

Damage to acceleration-sensitive non-structural components and contents is usually related to the peak (in time) of the SRSS of the floor accelerations in the two main orthogonal directions (PFA). The PFA is the peak of the “absolute (total)” floor acceleration. The maximum directionless peak floor acceleration at storey  $i$  is computed as:

$$PFA_i = \max\left(\sqrt{FA_{i,x}^2(t) + FA_{i,y}^2(t)}\right) \quad (14)$$

Where  $FA_{i,j}$  represents the floor acceleration at floor  $i$  in direction  $j$ .

As a single EDP for acceleration sensitive components the maximum directionless building floor acceleration is employed:

$$PFA = \max(PFA_1, \dots, PFA_n) \quad (15)$$

MIDR and PFA are selected for their simplicity and significance. However, if correlated to the damage of a specific component, any EDP extractable from the structural response could be employed. An example could be the spectral floor acceleration at a given period and floor.

Note that, as per definition of directionless PFA and MIDR, the corresponding way of computing the IM component leads to the estimation of the RotD100 component (Boore 2010).

## 5. Performance Levels selection

In order to generate fragility curves for MIDR and PFA, five performance levels are considered (ASCE 2014): Immediate Occupancy (IO), Damage Limitation (DL), Life Safety (LS), Collapse Prevention (CP) and Collapse (C).

For MIDR the assumed capacity thresholds  $edp_{pl}$  are identified by means of pushover analysis as follows:

- IO:  $edp_{IO} = 0.7\%$  - this threshold is equal to the MIDR that leads to the first appearance of damage in the structure, identified as the rebar yielding;
- DL:  $edp_{DL} = 1.0\%$  - identified as the MIDR that leads to the first unconfined concrete crushing;
- LS:  $edp_{LS} = 3.0\%$  - defined as  $\frac{3}{4} edp_{CP}$ ;
- CP:  $edp_{CP} = 4.0\%$  - evaluated as the MIDR at which the collapse chord rotation defined as per the Italian Building Code (C.S.LL.PP 2018) is attained;
- C:  $edp_C = 7.0\%$  - evaluated as the MIDR corresponding to a reduction of 20% of the maximum base shear.

For PFA the assumed thresholds  $edp_{pl}$  are as follows (Kohrangi et al. 2017):

- IO:  $edp_{IO} = 0.45$  g;
- DL:  $edp_{DL} = 0.55$  g;

- LS:  $edp_{LS} = 0.65$  g;
- CP:  $edp_{CP} = 0.75$  g;
- C:  $edp_C = 1.5$  g.

The thresholds for PFA have been selected arbitrarily as they could differ depending on the component to be analysed.

Moreover, since the aim is to evaluate the IMs up to collapse, several records may cause very large displacements or convergence problems due to large input accelerations, hence global collapse (Bakalis and Vamvatsikos 2018). These analyses need to be identified for an accurate fragility evaluation. The following criteria are adopted to identify collapsed analysis (Jalayer et al. 2015, 2017; Galanis and Moehle 2015; Kohrangi et al. 2016c, b; Ebrahimian and Jalayer 2021):

- The achievement of a MIDR greater than  $edp_C = 7\%$  (to account for dynamic instability);
- The loss of convergence of the analysis (after accurate inspection);
- The development of a floor mechanisms (50% of columns of one storey reach chord rotation capacity).

Theoretically, when a structure approaches dynamic instability displacements (hence EDP) approaches infinity therefore fragility can be evaluated considering an arbitrarily large EDP, well beyond the maximum non collapse case (Bakalis and Vamvatsikos 2018). In this study, a MIDR = 10% is assigned to non-convergence cases and collapsed analysis experiencing higher MIDRs.

## 6. Record selection

The number of records needed for the estimation of fragility curves usually varies between 40 and 100 depending on the selected method of evaluation (Hancock et al. 2008; Gehl et al. 2015; Baltzopoulos et al. 2018; Kiani et al. 2018). When adopting the cloud method for fragility evaluation, a few points should be considered (Jalayer et al. 2017):

- The records should cover a wide range for the selected IM;
- A significant number of records (about 20-30%) should lead to an exceedance of the selected EDP capacity for the selected performance level;
- No more than 10% of records from the same event should be selected.

In this study, records are selected from a database of simulated ground motions (Fasan and Barnaba 2021). Records are selected in order to have magnitudes ranging from 5.5. to 7 and expected macroseismic intensity  $I_{EMS,avg}$  ranging from 6 to 9. For each  $I_{EMS,avg}$  degree, 90 accelerograms are chosen leading to a total of 360 records. This selection criterion is adopted to assure that records cover a wide range of IMs, including  $I_{EMS}$ . Not particular care is given to focal mechanisms, distance or soil category since an objective is to test sufficiency. Distributions of magnitudes and distances are shown in Figure 3 and Figure 4.

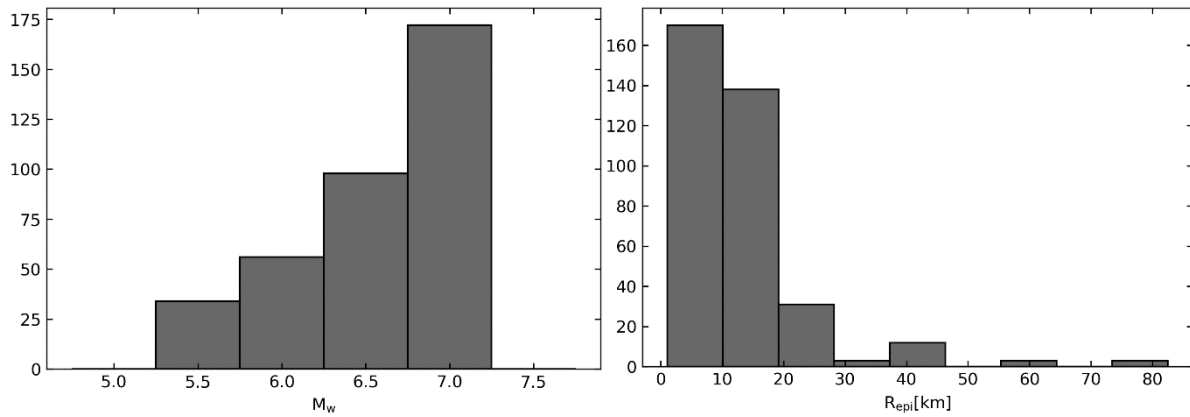


**Figure 3: Magnitude (left) and Distance (right) distribution of the selected records**

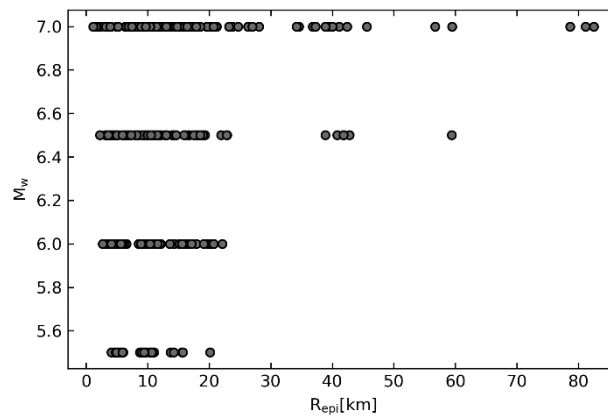


**Figure 4: Magnitude-distance scatter plot for the selected records**

In the performed 360 non linear time history analysis, the north component is always assigned to the x direction while the east component to the y direction. Given that the building was designed for moderate seismic action, the macroseismic intensity range, following the indications of Jalayer et al. (2017), was chosen accordingly. This range does not imply that the building will collapse under these signals, since this depends also on the characteristic on the building and not only on those of the signal. This is confirmed by the results obtained in the following sections where less than 60 signals out of 360 lead the structure to collapse

## 7. Methodology

### 7.1. Fragility development

Even with cloud analysis, when dealing with collapse cases, the original *IM-EDP* data pairs resulting from the *n* NLTHAs (corresponding to the initial set of data  $\mathbf{D} = [(IM_1, EDP_1), \dots, (IM_n, EDP_n)]$  – the “cloud”) can be subdivided in Collapse (C) and Non Collapse (NC) cases. With this separation, using the total probability theorem, the fragility function for a given performance level can be written as (Shome and Cornell 1999; Jalayer and Cornell 2009):

$$P(EDP > edp_{pl} | IM) = P(EDP > edp_{pl} | IM, NC)P(NC | IM) + P(C | IM) \quad (16)$$

Where  $P(EDP > edp_{pl} | IM, NC)$  is the probability of experiencing and *EDP* greater than *edp<sub>pl</sub>* given that collapse has not taken place (NC). This curve can be calculated with standard cloud analysis that supposes the following linear relation between the logarithm of *EDP* and the logarithm of *IM*:

$$\ln(edp|im) = a + b \cdot \ln(im) \quad (17)$$

Where  $\ln(edp|im)$  is a median estimate of the demand given the intensity measure value  $im$  and  $a$  and  $b$  are the model parameters than can be evaluated applying the Ordinary Least Square (OLS) method on the NC cases ( $n_{NC}$  NLTHAs). As per hypothesis of OLS, residuals around the mean value are normally distributed with zero mean and constant logarithmic standard deviation evaluated as:

$$\sigma_{\ln(EDP)|\ln(IM)} = \sqrt{\frac{\sum_1^n (\ln(EDP_i) - \ln(edp_i|IM_i))^2}{n_{NC} - 2}} \quad (18)$$

Therefore, given an  $EDP$  threshold  $edp_{pl}$ , the probability of experiencing an  $EDP$  grater than  $edp_{pl}$  given  $IM$  and  $NC$  follows a lognormal distribution and is given by the following relation:

$$P(EDP > edp_{pl}|IM, NC) = 1 - \Phi\left(\frac{\ln(edp_{pl}) - \ln(edp|im)}{\sigma_{\ln(EDP)|\ln(IM)}}\right) \quad (19)$$

Where  $\Phi$  is the standard normal cumulative distribution. The probability of collapse  $P(C|IM)$  can be predicted as a function of  $IM$  by the following logistic model (Jalayer et al. 2017):

$$P(C|IM) = \frac{1}{1 + e^{-(\alpha_0 + \alpha_1 \cdot \ln(im))}} \quad (20)$$

Where the model parameters  $\alpha_0$  and  $\alpha_1$  can be determined applying the maximum likelihood estimation method to the logistic model of Equation (20) to entire cloud data (n time history analysis). Logistic regression is used when the dependent variable is binary. In this case the dependent variable is going to be 1 when the structure collapses and 0 when the structure does not collapse. It is straightforward to see that the probability of non-collapse is:

$$P(NC|IM) = 1 - P(C|IM) = \frac{e^{-(\alpha_0 + \alpha_1 \cdot \ln(im))}}{1 + e^{-(\alpha_0 + \alpha_1 \cdot \ln(im))}} \quad (21)$$

Therefore, Equation (16) can be rewritten and the fragility function, considering collapse cases, assumes the following form:

$$P(EDP > edp_{pl}|IM) = \Phi\left(\frac{\ln(edp|im) - \ln(edp_{pl})}{\sigma_{\ln(EDP)|\ln(IM)}}\right) \frac{e^{-(\alpha_0 + \alpha_1 \cdot \ln(im))}}{1 + e^{-(\alpha_0 + \alpha_1 \cdot \ln(im))}} + \frac{1}{1 + e^{-(\alpha_0 + \alpha_1 \cdot \ln(im))}} \quad (22)$$

Hence, the fragility curve depends on the vector of 5 parameters  $\theta_F = [a, b, \sigma_{\ln(EDP)|\ln(IM)}, \alpha_0, \alpha_1]$ . The probability of experiencing an  $EDP$  lower than  $edp_i$  given  $IM$  (i.e. the CDF of  $EDP$ ) is given by:

$$P(EDP \leq edp_i|IM) = \Phi\left(\frac{\ln(edp_i) - a - b \cdot \ln(im)}{\sigma_{\ln(EDP)|\ln(IM)}}\right) \frac{e^{-(\alpha_0 + \alpha_1 \cdot \ln(im))}}{1 + e^{-(\alpha_0 + \alpha_1 \cdot \ln(im))}} \quad (23)$$

Finally, equation (23) can also be used to evaluate the regression curve and confidence intervals by setting the left side equal to the required percentile  $p$  and solving for  $edp_i$ :

$$\ln(edp_i)^p = a + b \cdot \ln(im_i) + \sigma_{\ln(EDP)|\ln(IM)} \cdot \Phi^{-1}\left(\frac{p}{P(NC|im_i)}\right) \quad (24)$$

Where  $\Phi^{-1}$  is the inverse of the standard normal cumulative distribution.

Generally speaking, fragility functions should be developed including the effect of uncertainties (Pitilakis et al. 2014; Bakalis and Vamvatsikos 2018; Silva et al. 2019):

- due to record-to-record variability;
- due to variability of the mechanical properties;
- due to variability of performance level capacity thresholds;
- due to model parameters.

The first three can be classified as mainly aleatory uncertainties, whereas the last one as mainly epistemic. Note that the vector of parameters  $\theta_F$  is a function of the initial cloud data  $\mathbf{D}$ . The followed methodology naturally accounts for record-to-record variability as each couple of  $\mathbf{D}$  comes from a different record. Moreover, even if not accounted for in this study, variability on mechanical properties could be accounted for by sampling, for each record, a different realization of the mechanical properties. Finally, in order to account for the epistemic uncertainty in the model parameters  $\theta_F$ , a bootstrap procedure can be applied (Iervolino 2017). This procedure relies on resampling with replacements the initial data, hence leading to  $n$  different realizations of  $\theta_F$  and consequently  $n$  fragility and regression curves. The number of bootstraps adopted is  $n = 1000$ . Note that, to account also for the variability in the performance level threshold,  $edp_{pl}$  could be added to the parameters vector  $\theta_F$  and take a different value for each realization. Summarizing, the combination of the modified cloud analysis (Jalayer et al. 2017) with the bootstrap procedure (Iervolino 2017) allows to evaluate the expected variability for the fragility curves including all sources of uncertainties. In this study, only record-to-record variability and model parameters uncertainties are accounted for.

## 7.2. Efficiency and proficiency evaluation

Efficiency is evaluated as the logarithmic standard deviation  $\sigma_{\ln(EDP)|\ln(IM)}$  of the linear regression shown in equation (17), i.e. the dispersion of EDPs given the IM. As this term is constant for the entire range of EDPs, it is not suitable for assessing near collapse cases, where EDPs approach infinity. Hence, it is evaluated only for the non collapse cases.

As an alternative measure able to evaluate results up to collapse, the dispersion associated to the median fragility curve is adopted. This measure is evaluated as follows (Jalayer et al. 2021):

$$\sigma_{\ln(IM)|\ln(EDP_{pl})} = 0.5 \cdot \ln \left( \frac{IM_{pl,50}^{84th}}{IM_{pl,50}^{16th}} \right) \quad (25)$$

Where  $M_{pl,50}^{84th}$  and  $M_{pl,50}^{16th}$  are the 84<sup>th</sup> and 16<sup>th</sup> percentile IM values evaluated on the median fragility (the median coming from the bootstrap procedure). In literature  $\sigma_{\ln(IM)|\ln(EDP)}$  is often referred as “proficiency” and for non-collapse cases it is equal to:

$$\sigma_{\ln(IM)|\ln(EDP_{pl})} = \frac{\sigma_{\ln(EDP)|\ln(IM)}}{b} \quad (26)$$

Note that  $\sigma_{\ln(IM)|\ln(EDP)}$  assumes different values for different performance levels, hence allowing to estimate the performance of the IM for each of them, ranging from linear to non-linear behavior.

### 7.3. Sufficiency

Sufficiency is usually checked through linear regression between the predicted  $\ln(edp|im)$  and an independent seismological parameter  $S_i$ :

$\ln(edp im) = a + b \cdot S_i$	(27)
---------------------------------	------

Here, moment magnitude  $M_w$ , logarithm of epicentral distance  $\ln(R_{epi})$  and logarithm of the average shear wave velocity  $\ln(V_{s,30})$  are considered separately.

A sufficient measure should be independent from  $S_i$ . Generally, independence is evaluated by the level of statistical significance of the hypothesis that the slope  $b$  of the regression is zero (i.e. no dependence of  $\ln(edp|im)$  on  $S_i$ ). This is evaluated by the p-value, i.e. the probability that the slope is different from zero. A small p-value indicates that it is not possible to state that there is independence whereas high p-value indicates that it is not possible to say that there is dependence. However, for a complete view also slope  $b$ , the standard deviation  $\sigma$  of the regression and  $R^2$  values are reported. In fact, even with an low p-value, the magnitude of the influence may be negligible from a practical point of view and the regressions parameters can tell more about this influence (Kazantzi and Vamvatsikos 2015).

## 8. Results and discussion

### 8.1. Efficiency and proficiency

Efficiency and proficiency are evaluated as indicated in section 7.2. Figure 5: Efficiency for the selected IMs: MIDR (top) and PFA (bottom). Figure 5 shows the efficiency results for the 22 IMs evaluated for MIDR and PFA. As it can be seen,  $I_{EMS}$  is the less efficient measure meaning that, given an  $I_{EMS}$  value, there is a high dispersion of the results around the mean. In practice this means that a higher number of records is needed to estimate the median  $EDP$  when using  $I_{EMS}$ . The most efficient measure for MIDR is  $PSA_{avg,GMRotD50}$ , whereas  $PGA_{RotD100}$  is the most efficient measure for PFA estimation. Note that PFA and  $PGA_{RotD100}$  have basically the same definition and they differ by the filter effect of the structure.  $I_{EMS,avg}$  shows intermediate results both for MIDR and PFA.

Proficiency evaluation is here reported only for the Life Safety and the Collapse Performance Levels, whereas the complete results can be found in APPENDIX 2. Figure 6 shows that, as expected, proficiency is lower closer to collapse. Moreover, for both MIDR and PFA, the measure that shows the highest proficiency is  $I_{EMS,avg}$ . As reported in the introduction, proficiency is a combination of efficiency and practicality (Padgett et al. 2008). This result is hence due to the elevated slope  $b$  of  $I_{EMS,avg}$  with respect to the other intensity measures. Due to an elevated slope also  $I_{EMS}$  shows a good proficiency for both MIDR and PFA with values comparable with  $PSA_{avg,GMRotD50}$ . This trend is visible both for the LS performance level and C performance level.

Among the commonly used IMs,  $PSA_{avg,GMRotD50}$  shows the higher efficiency for MIDR whereas  $PGA_{RotD100}$  for PFA. As regard the selection of the ground motion component it seems that there is not a significant difference between in the results meaning that any bidirectional component could be used.



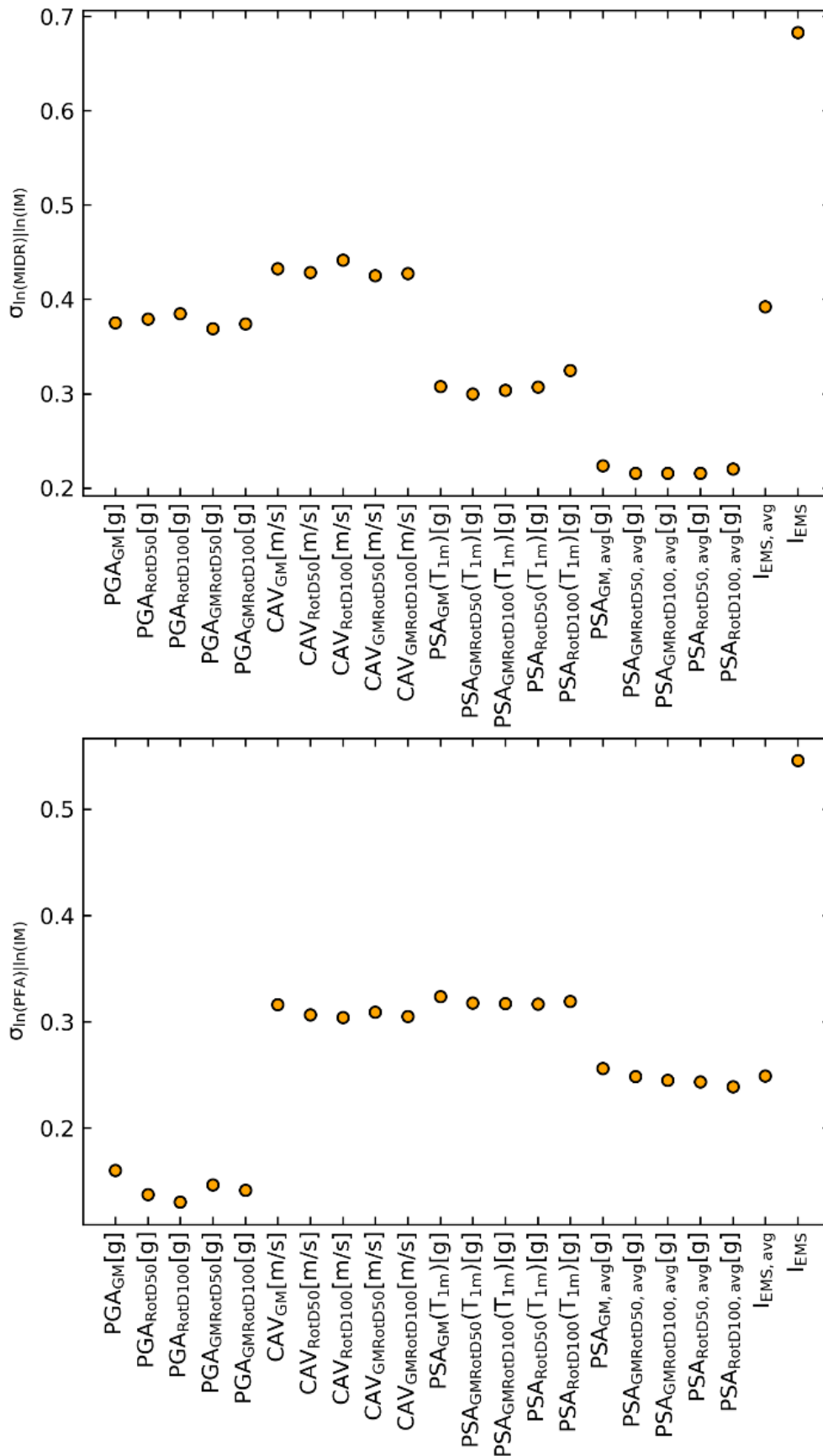


Figure 5: Efficiency for the selected IMs: MIDR (top) and PFA (bottom)

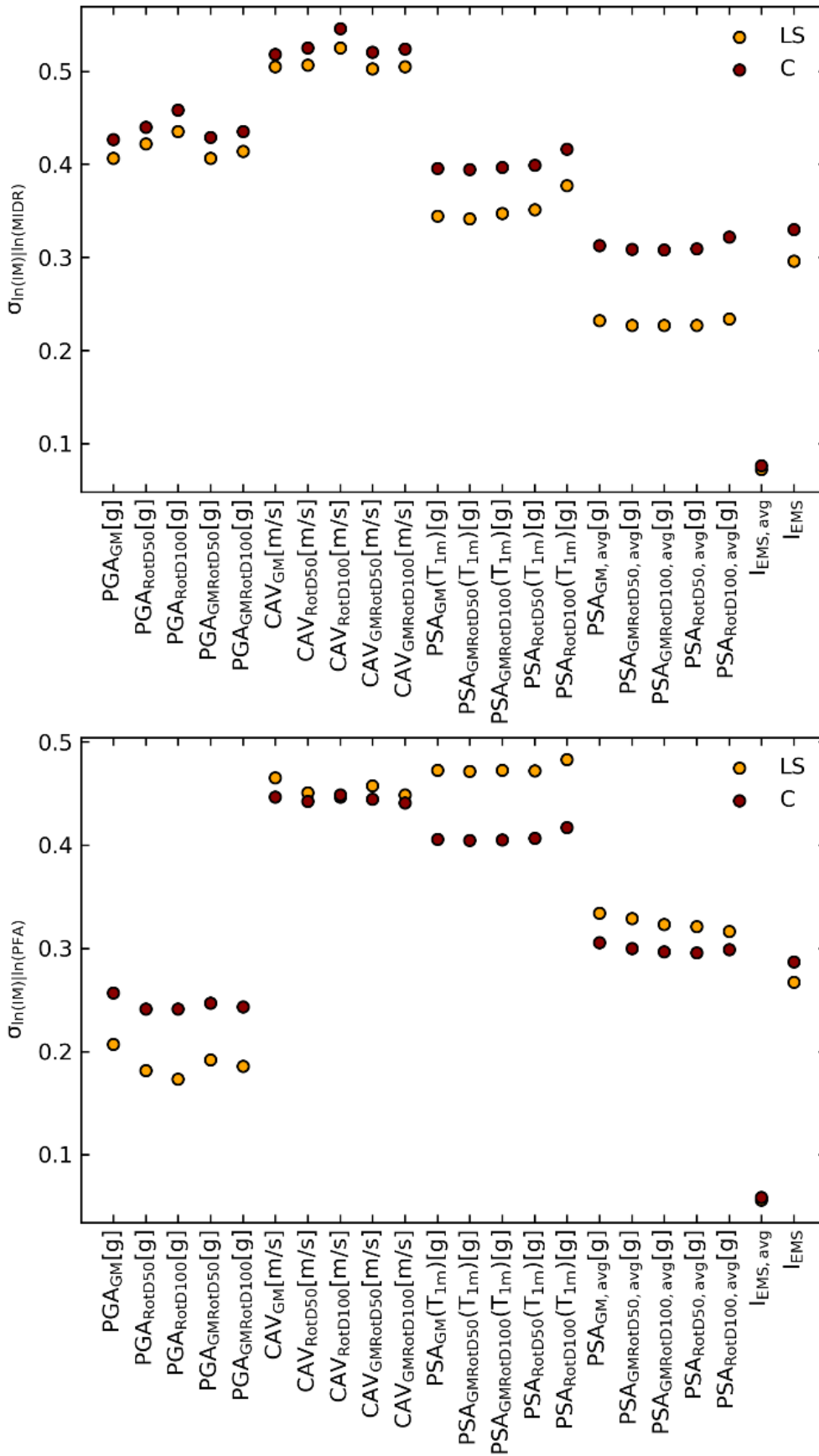


Figure 6: Proficiency for the selected IMs: MIDR (top) and PFA (bottom)

## 8.2. Sufficiency

Sufficiency results are reported in detail in APPENDIX 2. For the entire range of considered IMs the p-value is practically zero. This indicates that it is not possible to say that there is independence between the IMs and the investigated seismological parameters. To better understand the level of dependence, Figure 7 to Figure 12 report the absolute value of the estimated slope  $b$ , the standard deviation of the regression and the R-squared value for both MIDR and PFA. The value of the slope indicates the level of influence of the parameters, whereas the standard deviation indicates the level of dispersion. The R-squared value gives an indication of the amount of variability in the dependent variable explained by the independent variable. Analysing Figure 7 to Figure 9, it can be seen that for MIDR the slope ranges from 0.5 to 0.7 for most of the IMs both for moment magnitude and average shear velocity. For epicentral distance slope ranges between 0.2 and 0.4. Notable exceptions are the CAV that shows a slope around 0.9 for moment magnitude and  $I_{EMS}$  that on the contrary seems to be the most sufficient measure for MIDR with slopes around 0.2 for all the considered seismological parameters. The r-squared value is always under 0.2 with the exception of CAV and the lower value is again registered for  $I_{EMS}$ . Similar considerations can be done for PFA analyzing Figure 10 to Figure 12. Given the results it could be argued that not much can be gained in terms of explanatory power adding these seismological parameters in the regression model. Among the analyzed intensity measures,  $I_{EMS}$  seems to be the IM that shows the highest level of independence from the seismological parameters. This result seems in contrast with the findings of  $I_{EMS,avg}$ . As reported by other authors (Kazantzi and Vamvatsikos, 2015), the inefficiency of an intensity measure can create noise that prevents a clear dependence on the seismological parameters from being detected and this could be the reason for the apparent better performance of  $I_{EMS}$ .

The differences obtained between PGA and CAV, which are usually highly correlated IMs (Campbell and Bozorgnia 2019), were also reported by other authors (Ebrahimian et al. 2015; Ebrahimian and Jalayer 2021) and may be due to the presence of pulse-like records in the selected dataset.

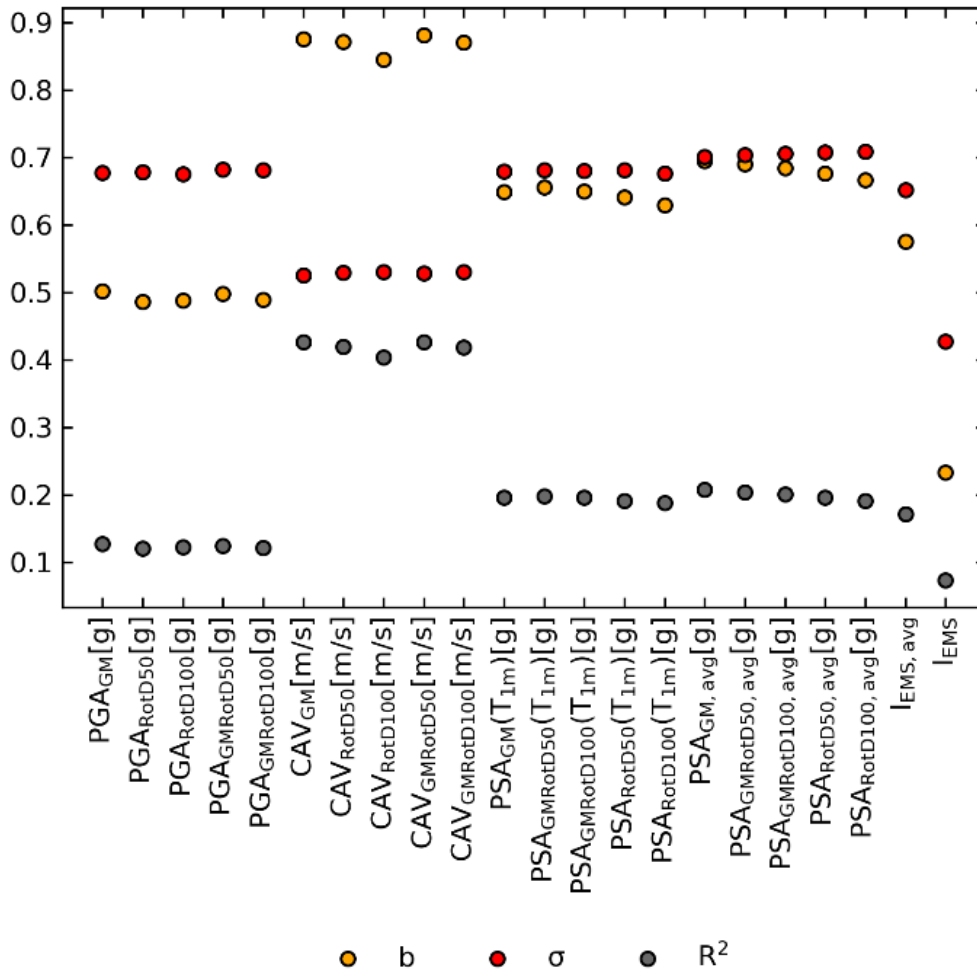


Figure 7: sufficiency results for MIDR: Mw

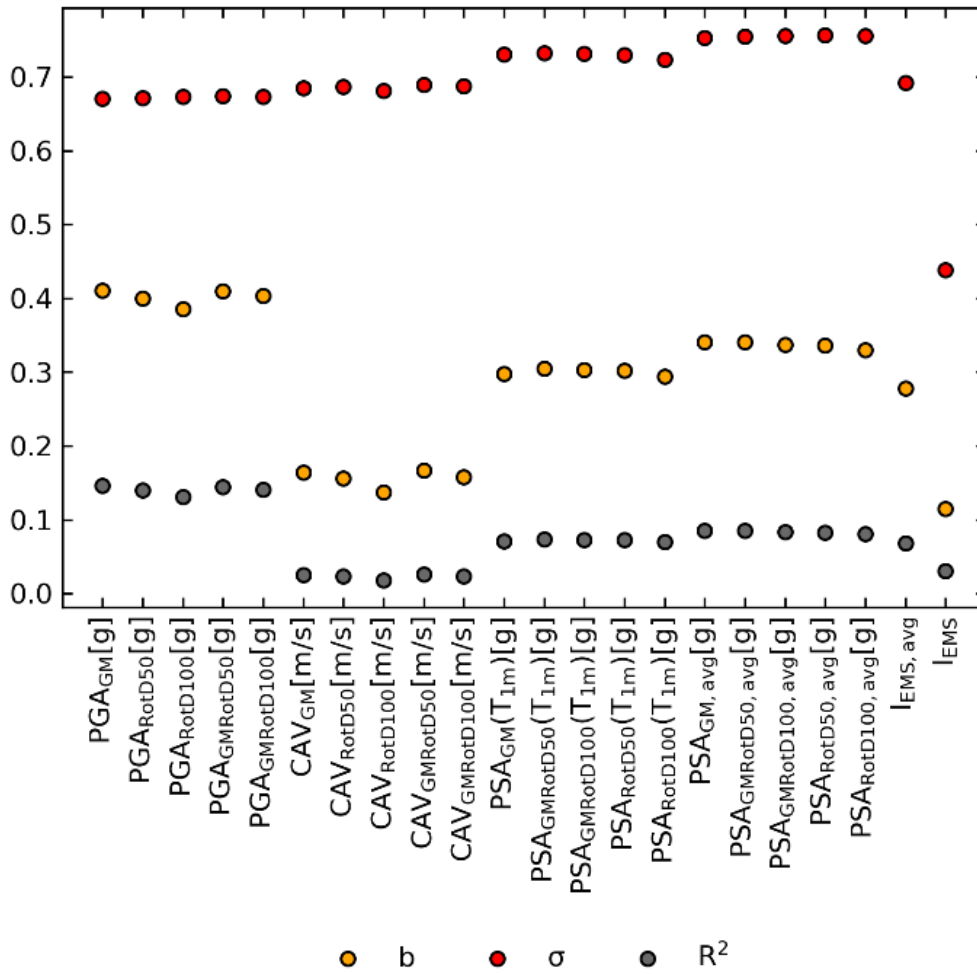


Figure 8: sufficiency results for MIDR: Repl

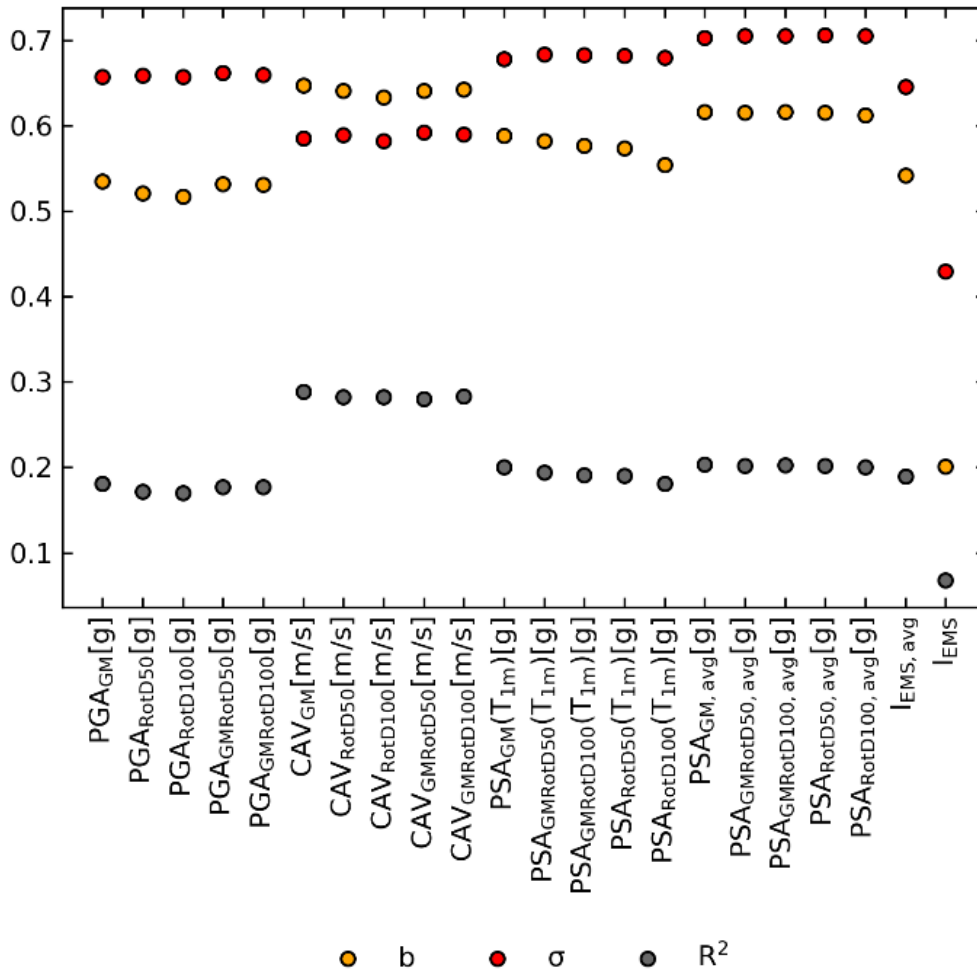


Figure 9: sufficiency results for MIDR: Vs,30

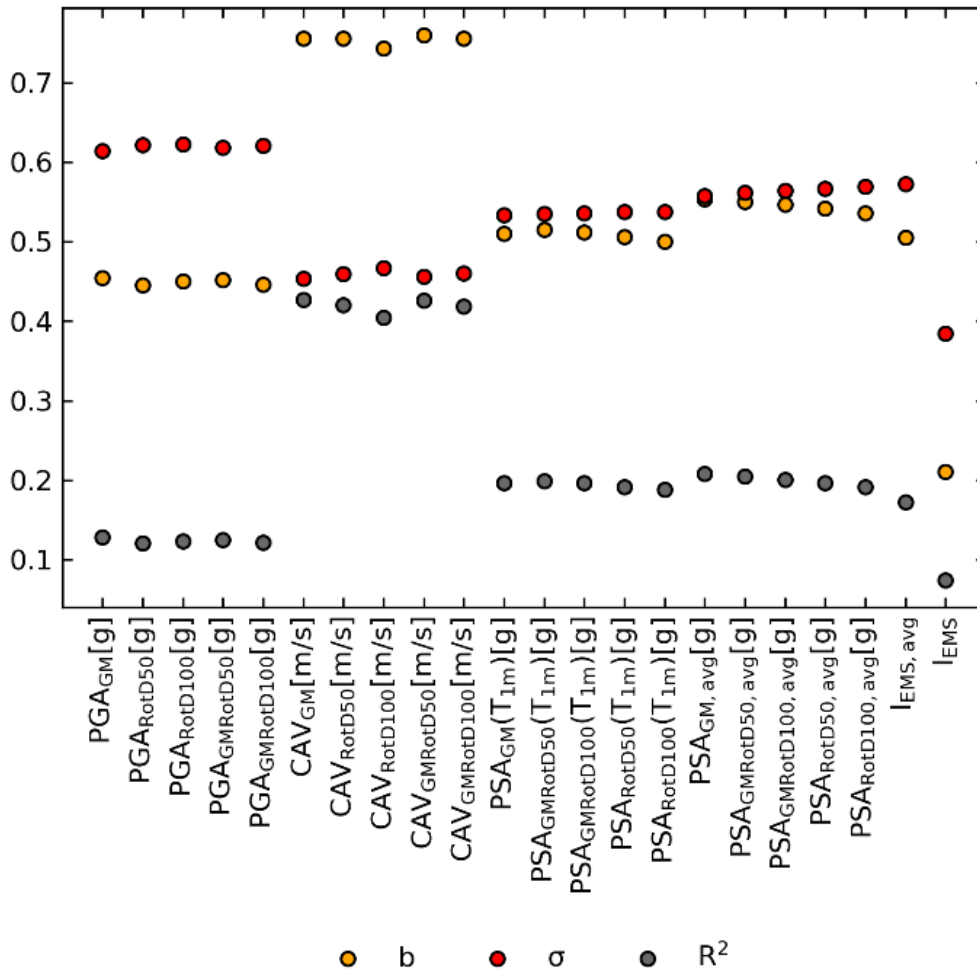


Figure 10: sufficiency results for PFA: Mw

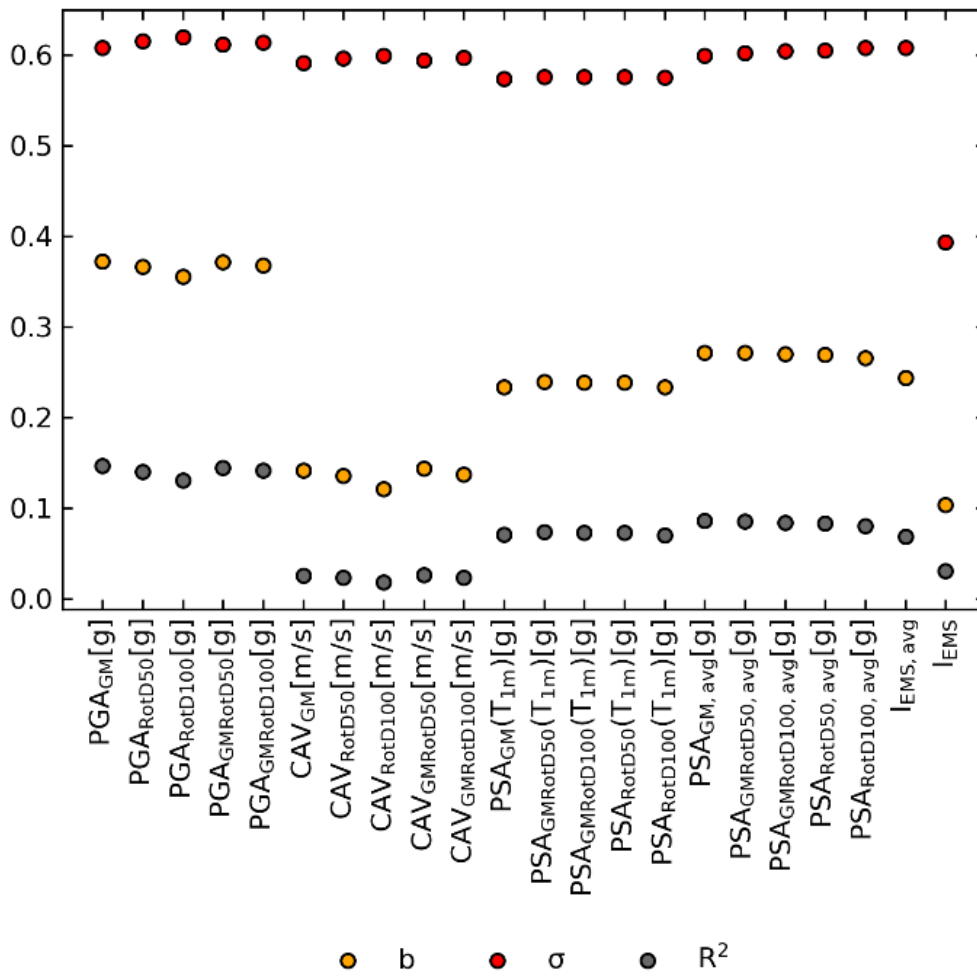


Figure 11: sufficiency results for PFA: Repl



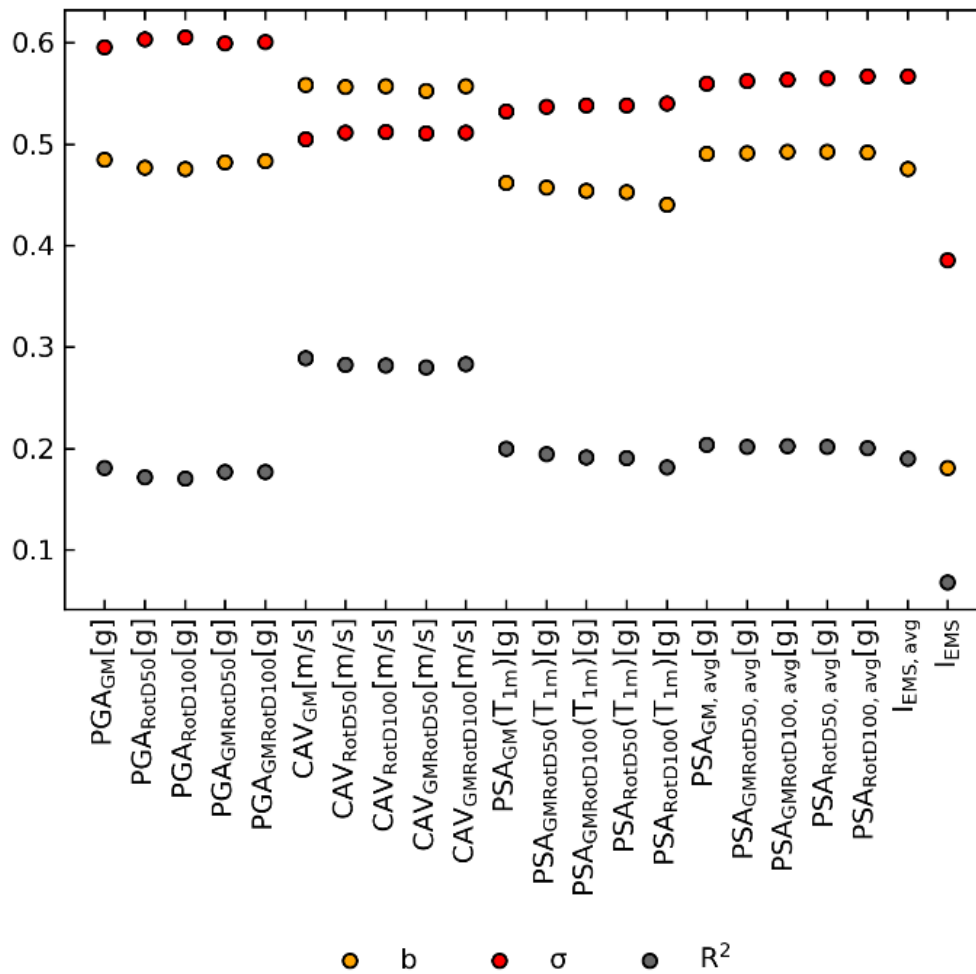


Figure 12: sufficiency results for PFA: Vs,30

### 8.3. Regression curves

The methodology shown in the previous sections is here applied to the 22 selected intensity measures. For the sake of brevity only the fragility functions for  $PSA_{avg,GMRotD50}$ ,  $I_{EMS}$  and  $I_{EMS,avg}$  are shown in detail whereas results for the other IMs are reported in appendixes.  $PSA_{avg,GMRotD50}$  is selected for comparison with  $I_{EMS}$  and  $I_{EMS,avg}$  since it is among the IMs that give the best results.

Figure 13, Figure 14 and Figure 15 show the regression curves for the three IMs. In the pictures the median regression values and the confidence interval for the prediction are shown. Non collapse IM-EDP couples are shown with grey dots whereas collapse cases with red dots. The median estimated parameters from the bootstrap analysis are also reported and light grey lines show the single bootstrap corresponding to a realization of the vector  $\theta_F$ . As it can be seen,  $PSA_{avg,GMRotD50}$  shows less scatter around the mean whereas  $I_{EMS}$  and  $I_{EMS,avg}$  show higher dispersions but also a higher slope, as also pointed out in section 8.1. All the regression curves become flat as EDPs approach the collapse value, indicating that collapses are effectively accounted for by the assumed model.

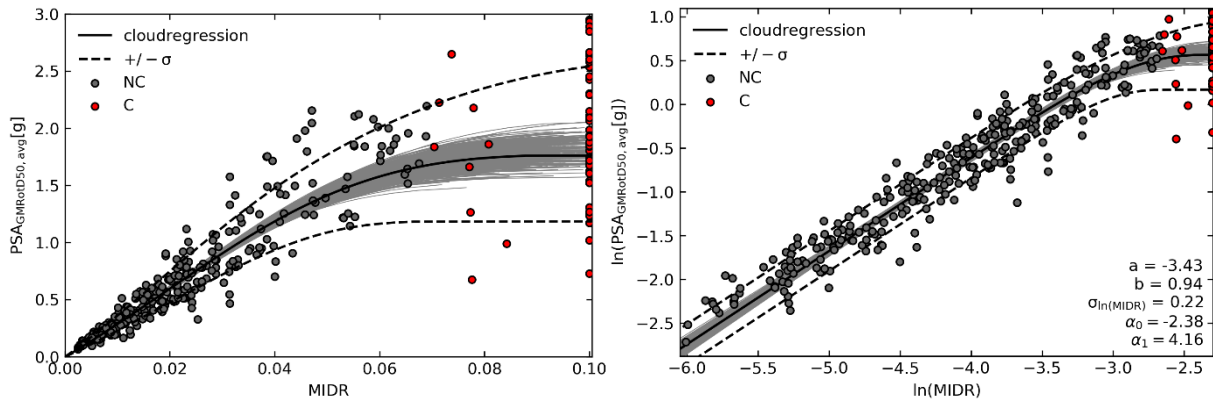


Figure 13: Regression curves for  $PSA_{avg,GMRotD50}$ : linear scale (left) and logarithmic scale (right)

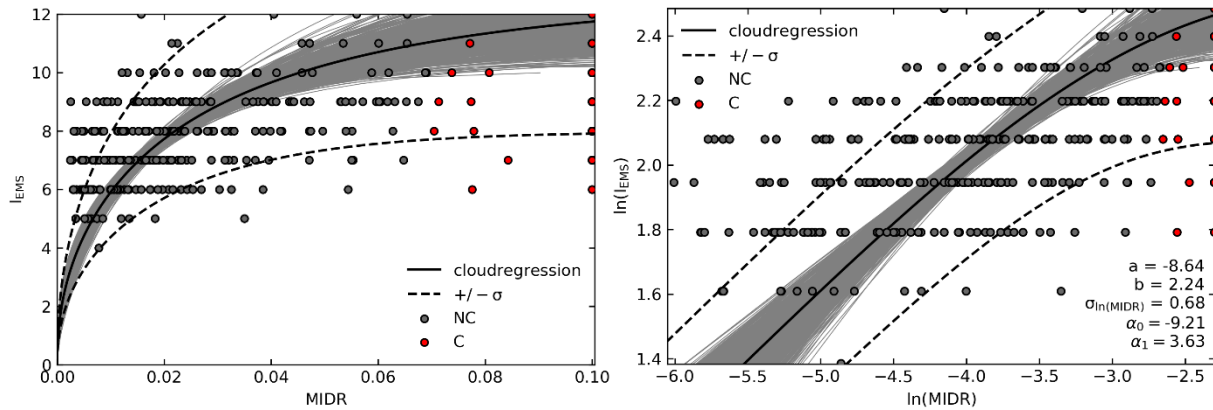


Figure 14: Regression curves for  $I_{EMS}$  linear scale (left) and logarithmic scale (right)

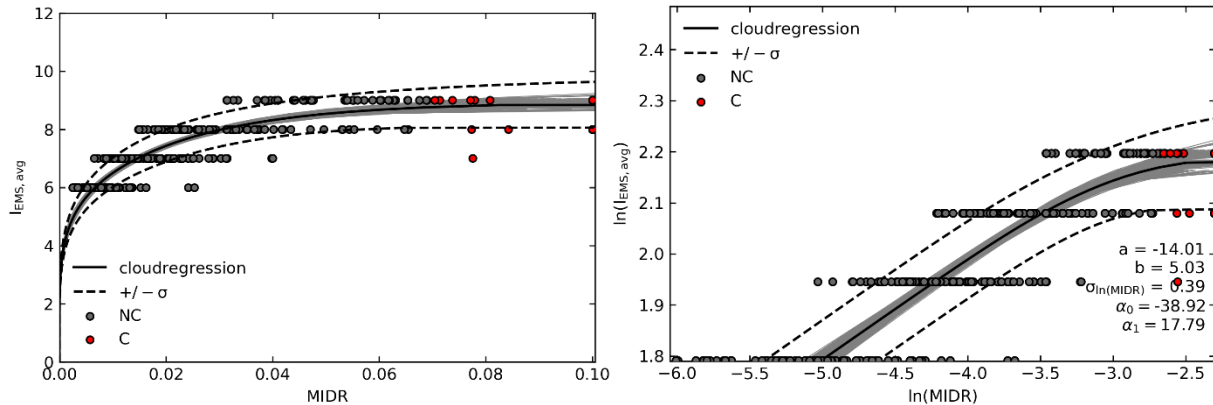


Figure 15: Regression curves for  $I_{EMS,avg}$  linear scale (left) and logarithmic scale (right)

Figure 16 and Figure 17 show, for  $PSA_{avg,GMRotD50}$  and  $I_{EMS}$ , the distribution of the five parameters defining the fragility functions resulting from the bootstrap analysis. As expected the parameters  $a$ ,  $b$  and  $\sigma_{\ln(EDP)|\ln(IM)}$  of the linear regression follow a normal distribution whereas the distribution of the parameters  $\alpha_0$  and  $\alpha_1$  of the logistic regression follow different distributions for different IMs. It should be noted that the five parameters are evaluated for each sample, therefore the possible correlation between collapse and non collapse cases is automatically accounted for. Figure 16 and Figure 17 show also the distribution of residual obtained by the regression model. Both  $PSA_{avg,GMRotD50}$  and  $I_{EMS}$  show normally distributed residuals.

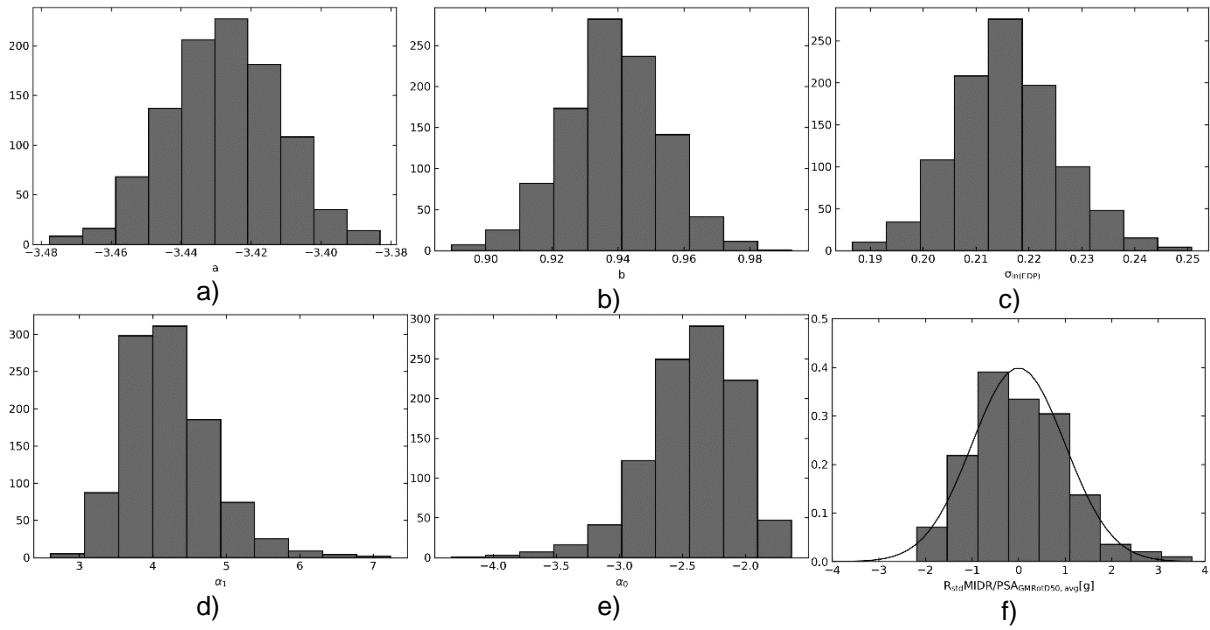


Figure 16: Distributions of fragility parameters from bootstrap analysis (a to e) and residuals from regression analysis (f) for  $PSA_{avg,GMRotD50}$

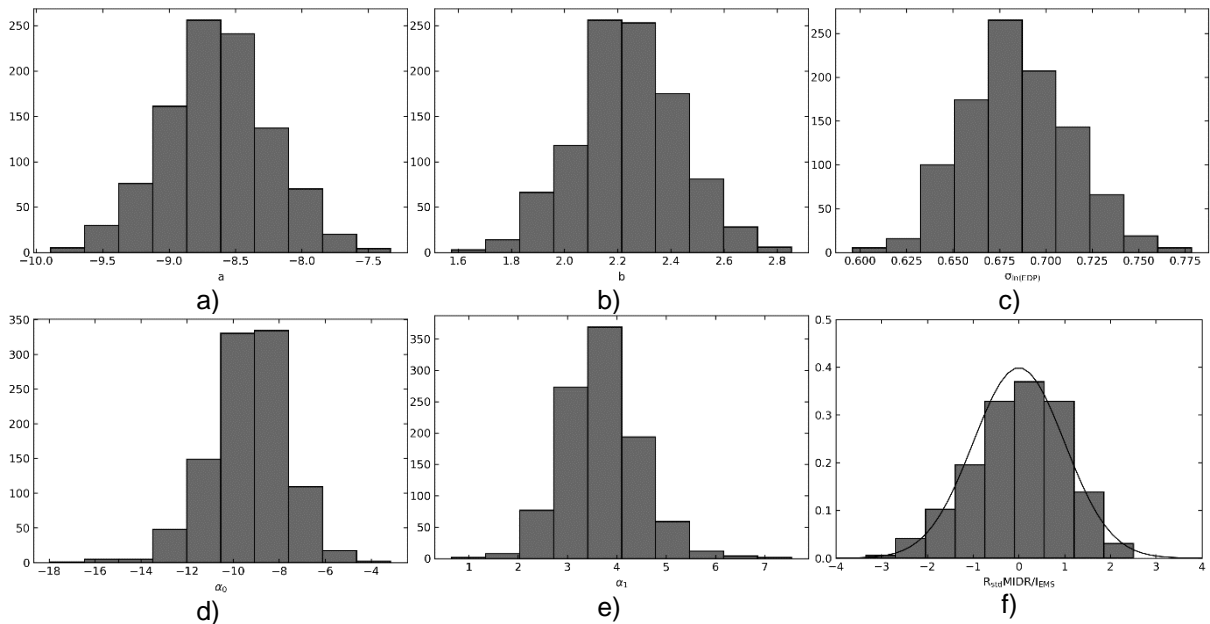


Figure 17: Distributions of fragility parameters from bootstrap analysis (a to e) and residuals from regression analysis (f) for  $I_{EMS}$

### 8.1. Fragility functions

Fragility functions for  $PSA_{avg,GMRotD50}$ ,  $I_{EMS}$  and  $I_{EMS,avg}$  are shown in Figure 18, Figure 19 and Figure 20 respectively. The fragility functions are shown only for the Life Safety and the Collapse performance levels whereas the median values of the estimated parameters for the 22 IMs are reported in APPENDIX 1.

Note that  $\sigma_{\ln(IM)|\ln(EDP_{pl})}$  used as a metric to evaluate proficiency and evaluated with equation (25) can also be seen as the standard deviation of a lognormal fragility equivalent to the five-parameter non-lognormal fragility defined by equation (22). IMs with better proficiency show lower standard deviations  $\sigma_{\ln(IM)|\ln(EDP_{pl})}$ , hence steeper fragility curves. Lower standard deviation of the fragility curves means

higher confidence in the median IM value leading to the exceedance of the performance level. The uncertainty around the median value (the width of the grey band) increases passing from the life safety to the collapse performance level. This is due to the widening of the confidence interval of the mean value as we move away from the average value of IM and can be seen also in the regression curves.

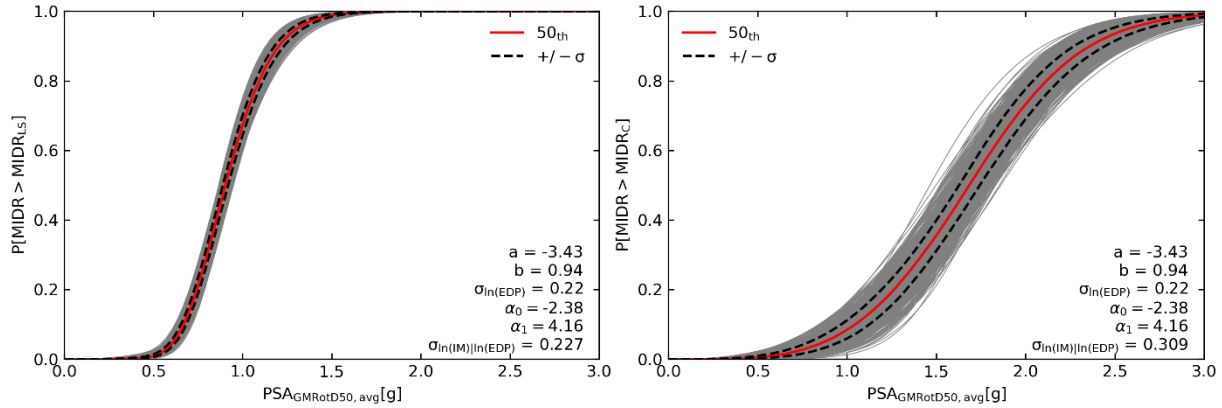


Figure 18:  $PSA_{avg,GMROT50}$  based fragility functions: Life Safety (left) and Collapse (right)

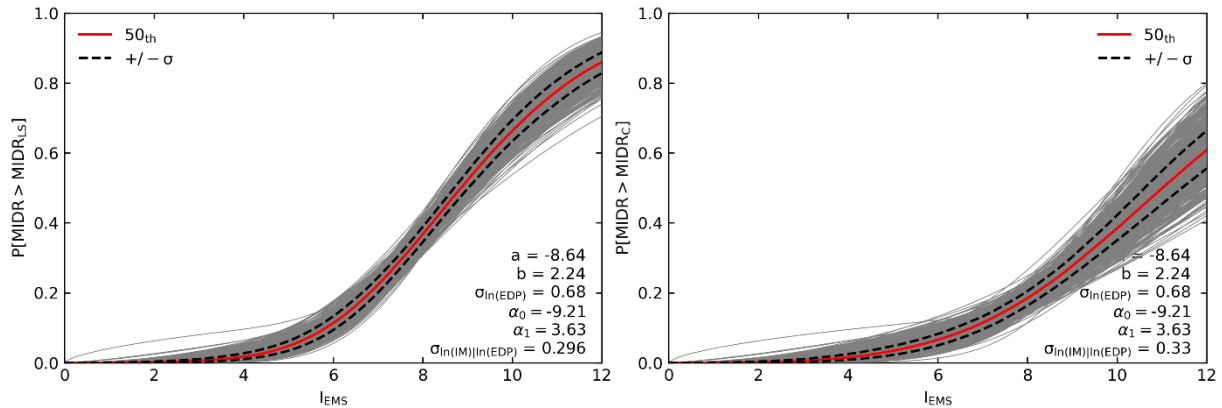


Figure 19:  $I_{EMS}$  based fragility functions: Life Safety (left) and Collapse (right)

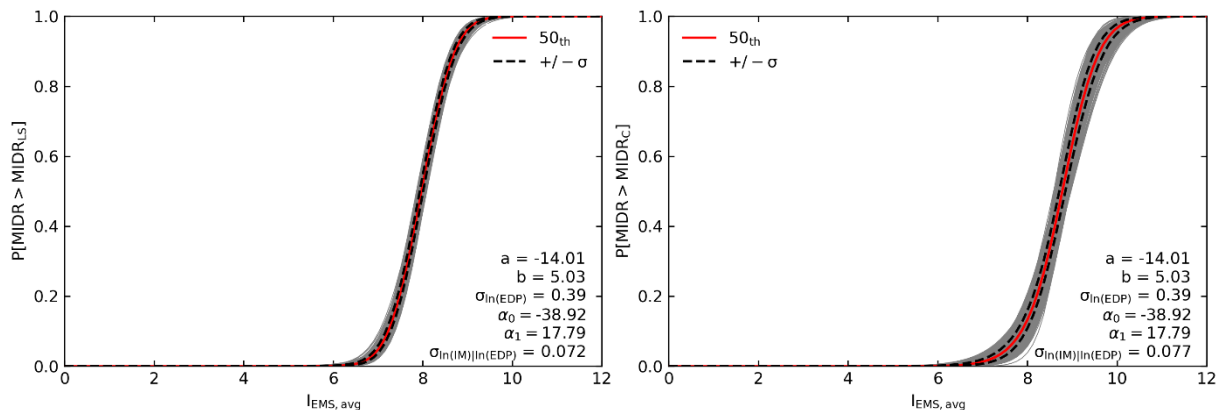


Figure 20:  $I_{EMS, avg}$  based fragility functions: Life Safety (left) and Collapse (right)

Differences in the fragility function developed on  $I_{EMS}$  and  $I_{EMS, avg}$  may be due to the fact that  $I_{EMS, avg}$  ignores the distribution of kinematic ductility values associated with a degree of intensity. The higher the dispersion, therefore the lower the efficiency, and the more the fragility curves flatten, increasing the probabilities for values lower of the median and reducing them for higher values. This seems to be confirmed by the fact that the median  $I_{EMS}$  and  $I_{EMS, avg}$  capacity is similar.

## 8.2. Validity of results

All the results presented in previous sections are obtained sampling physics-based simulated accelerograms from a previously assembled database (Fasan and Barnaba 2021). Each record is assigned an “instrumental”  $I_{EMS}$  based on equation (8) developed in Fasan (2020). The main reason from selecting records from this database is that it is easier to create homogenous samples with a considerable amount of signals leading to collapse. This is due to the high number of simulated events included in database. In this section a comparison between results obtained from simulated and real signals (with given real  $I_{EMS}$ , i.e. assigned on the field) is performed. The reason is twofold:

- Firstly, to check if results from real records are equivalent to results from simulated records;
- Secondly, to verify if the assignment of an “instrumental”  $I_{EMS}$  with equation (8) is effectively able to reproduce real  $I_{EMS}$  values.

For this purpose real records are selected from a database of intensity-based real records (Fasan 2020) and synthetic records selected on section 6 are resampled. The same number of records (equal to 53) is used and synthetic records are selected trying to match the distribution of magnitudes and macroseismic intensities of the database of real records. The adequacy is evaluated by the level of statistical significance of the difference of the slopes between real and synthetic results. Slopes are evaluated as the median values coming from a bootstrap analysis. Linear regression is used (equation (17) - standard cloud analysis) since it is not possible to find real records causing collapse. The significance is evaluated by the p-value. A high p-value means no significant difference whereas a low p-value means significant difference. The confidence interval for significance is set to 95%. Table 2 reports the values for MIDR and Table 3 for PFA. No statistically significant difference is identified for MIDR for all the considered IMs, meaning that results from synthetic signals are similar to results from real signals. For PFA a statistically significant difference is highlighted for IMs based on spectral acceleration values. On the contrary, a high p-values is found for the other IMs. More than a real difference between synthetic and real signals, this could be due to some spectral shape effect present in real signals. In fact, 28 out of 53 selected real signals are coming from the 30<sup>th</sup> of October 2016 Central Italy event and this is not a good selection practice as highlighted in section 6. However, it was not possible to select them otherwise because, as mentioned, few real records with given  $I_{EMS}$  are available.

For both MIDR and PFA there is no statistical difference between the in “instrumental”  $I_{EMS}$  and the real one, meaning that equation (8) is a valid instrument to assign macroseismic intensity matching real observed variability.

**Table 2: Evaluation of equivalency between real and synthetic records - MIDR**

<i>IM</i>	$b_{sim}$	$\sigma_{b_{sim}}$	$b_{real}$	$\sigma_{b_{real}}$	<i>t</i> – stat	<i>p</i> – value	<i>significant</i>
$PGA_{GM}$	0.896	0.057	1.171	0.166	-1.561	0.122	NO
$PGA_{RotD50}$	0.888	0.054	1.142	0.168	-1.435	0.154	NO
$PGA_{RotD100}$	0.887	0.052	1.101	0.160	-1.268	0.208	NO
$PGA_{GMRotD50}$	0.907	0.055	1.169	0.165	-1.506	0.135	NO
$PGA_{GMRotD100}$	0.902	0.054	1.159	0.163	-1.492	0.139	NO
$CAV_{GM}$	0.829	0.072	1.014	0.182	-0.944	0.347	NO
$CAV_{RotD50}$	0.824	0.072	1.014	0.181	-0.976	0.331	NO
$CAV_{RotD100}$	0.805	0.075	1.004	0.178	-1.028	0.306	NO
$CAV_{GMRotD50}$	0.827	0.071	1.017	0.182	-0.970	0.334	NO
$CAV_{GMRotD100}$	0.827	0.072	1.019	0.181	-0.990	0.324	NO
$PSA_{GM}$	0.944	0.059	0.910	0.049	0.445	0.658	NO
$PSA_{RotD50}$	0.944	0.056	0.912	0.050	0.431	0.667	NO
$PSA_{RotD100}$	0.941	0.056	0.914	0.048	0.372	0.710	NO
$PSA_{GMRotD50}$	0.938	0.057	0.900	0.048	0.504	0.616	NO
$PSA_{GMRotD100}$	0.914	0.062	0.889	0.046	0.323	0.747	NO
$PSA_{avg,GM}$	1.016	0.062	1.097	0.044	-1.064	0.290	NO
$PSA_{avg,RotD50}$	1.028	0.060	1.100	0.042	-0.982	0.328	NO
$PSA_{avg,RotD100}$	1.029	0.059	1.097	0.043	-0.939	0.350	NO
$PSA_{avg,GMRotD50}$	1.028	0.058	1.093	0.042	-0.905	0.368	NO
$PSA_{avg,GMRotD100}$	1.021	0.057	1.079	0.040	-0.836	0.405	NO
$I_{EMS}$	2.407	0.681	2.466	0.659	-0.062	0.951	NO

**Table 3: Evaluation of equivalency between real and synthetic records - PFA**

<i>IM</i>	$b_{sim}$	$\sigma_{b_{sim}}$	$b_{real}$	$\sigma_{b_{real}}$	<i>t - stat</i>	<i>p - value</i>	<i>significant</i>
$PGA_{GM}$	0.790	0.025	0.789	0.049	0.024	0.981	NO
$PGA_{RotD50}$	0.775	0.024	0.791	0.047	-0.302	0.764	NO
$PGA_{RotD100}$	0.778	0.022	0.756	0.045	0.433	0.666	NO
$PGA_{GMRotD50}$	0.770	0.025	0.793	0.047	-0.413	0.681	NO
$PGA_{GMRotD100}$	0.779	0.024	0.788	0.046	-0.181	0.856	NO
$CAV_{GM}$	0.673	0.045	0.600	0.085	0.751	0.454	NO
$CAV_{RotD50}$	0.690	0.043	0.601	0.084	0.947	0.346	NO
$CAV_{RotD100}$	0.695	0.043	0.603	0.082	0.983	0.328	NO
$CAV_{GMRotD50}$	0.676	0.043	0.602	0.085	0.780	0.437	NO
$CAV_{GMRotD100}$	0.689	0.043	0.604	0.084	0.899	0.371	NO
$PSA_{GM}$	0.630	0.059	0.378	0.045	3.408	0.001	YES
$PSA_{RotD50}$	0.618	0.058	0.378	0.046	3.265	0.001	YES
$PSA_{RotD100}$	0.616	0.057	0.378	0.045	3.278	0.001	YES
$PSA_{GMRotD50}$	0.621	0.056	0.373	0.045	3.445	0.001	YES
$PSA_{GMRotD100}$	0.608	0.054	0.363	0.044	3.505	0.001	YES
$PSA_{avg,GM}$	0.735	0.046	0.486	0.045	3.880	0.000	YES
$PSA_{avg,RotD50}$	0.713	0.045	0.485	0.045	3.559	0.001	YES
$PSA_{avg,RotD100}$	0.717	0.045	0.485	0.045	3.662	0.000	YES
$PSA_{avg,GMRotD50}$	0.720	0.045	0.482	0.045	3.771	0.000	YES
$PSA_{avg,GMRotD100}$	0.720	0.043	0.477	0.043	3.999	0.000	YES
$I_{EMS}$	1.284	0.464	1.679	0.301	-0.713	0.477	NO

## 9. Conclusions and future works

In this deliverable the European Macroseismic Intensity  $I_{EMS}$  and its expected value  $I_{EMS,avg}$  are tested as Intensity Measures candidates for use in seismic risk analysis. In comparison with commonly used IMs,  $I_{EMS}$  shows lower efficiency but comparable proficiency (meaning that the dispersion of the fragility functions is similar).  $I_{EMS,avg}$  seems to show comparable efficiency and better proficiency. Overall,  $I_{EMS}$  seems to be the most sufficient measure among those compared in this study. The use of physics-based simulated signals and the assignment of an “instrumental”  $I_{EMS}$  does not lead to a significant difference compared with results obtained with real records. It is worth nothing that the evaluation of seismic risk through equation (2) (Cornell and Krawinkler 2000) depends on uncertainties related both to hazard and fragility assessment, therefore a reduction of response dispersion (better efficiency) or fragility curves standard deviation (proficiency) does not necessarily mean on overall reduction of risk variability.

In the future this study has to be extended including the influence of different building typologies and using different databases for record selections. Moreover, to better understand the suitability of  $I_{EMS}$  for seismic risk analysis, it is necessary to extend this study to a complete seismic risk analysis.



## Bibliography

- ASCE (2014) Seismic Evaluation and Retrofit of Existing Buildings. American Society of Civil Engineers, Reston, VA
- Bakalis K, Vamvatsikos D (2018) Seismic Fragility Functions via Nonlinear Response History Analysis. *Journal of Structural Engineering (United States)* 144:1–15. doi: 10.1061/(ASCE)ST.1943-541X.0002141
- Baker JW (2015) Efficient analytical fragility function fitting using dynamic structural analysis. *Earthquake Spectra* 31:579–599. doi: 10.1193/021113EQS025M
- Baker JW, Cornell CA (2005) A vector-valued ground motion intensity measure consisting of spectral acceleration and epsilon. *Earthquake Engineering and Structural Dynamics* 34:1193–1217. doi: 10.1002/eqe.474
- Baltzopoulos G, Baraschino R, Iervolino I (2018) On the number of records for structural risk estimation in PBEE. *Earthquake Engineering and Structural Dynamics* 1–18. doi: 10.1002/eqe.3145
- Bazzurro P, Cornell CA, Shome N, Carballo JE (1998) Three Proposals for Characterizing MDOF Nonlinear Seismic Response. *Journal of Structural Engineering* 124:1281–1289. doi: 10.1061/(ASCE)0733-9445(1998)124:11(1281)
- Boore DM (2010) Orientation-independent, nongeometric-mean measures of seismic intensity from two horizontal components of motion. *Bulletin of the Seismological Society of America* 100:1830–1835. doi: 10.1785/0120090400
- Boore DM, Watson-Lamprey J, Abrahamson NA (2006) Orientation-independent measures of ground motion. *Bulletin of the Seismological Society of America* 96:1502–1511. doi: 10.1785/0120050209
- C.S.LL.PP (2018) Norme tecniche per le costruzioni. Rome, Italy
- Campbell KW, Bozorgnia Y (2019) Ground Motion Models for the Horizontal Components of Arias Intensity (AI) and Cumulative Absolute Velocity (CAV) Using the NGA-West2 Database. *Earthquake Spectra* 35:1289–1310. doi: 10.1193/090818EQS212M
- Chieffo N, Fasan M, Romanelli F, et al (2021) Physics-Based Ground Motion Simulations for the Prediction of the Seismic Vulnerability of Masonry Building Compounds in Mirandola (Italy). *Buildings* 11:667. doi: 10.3390/buildings11120667
- Cornell BYCA (1968) Engineering Seismic Risk Analysis. *Bulletin of the Seismological Society of America* 58:1583–1606
- Cornell CA, Krawinkler H (2000) Progress and Challenges in Seismic Performance Assessment
- Eads L, Miranda E, Lignos DG (2015) Average spectral acceleration as an intensity measure for collapse risk assessment. *Earthquake Engineering & Structural Dynamics* 44:2057–2073. doi: 10.1002/eqe.2575
- Ebrahimian H, Jalayer F (2021) Selection of seismic intensity measures for prescribed limit states using alternative nonlinear dynamic analysis methods. *Earthquake Engineering and Structural Dynamics* 50:1235–1250. doi: 10.1002/eqe.3393
- Ebrahimian H, Jalayer F, Lucchini A, et al (2015) Preliminary ranking of alternative scalar and vector intensity measures of ground shaking. *Bulletin of Earthquake Engineering* 13:2805–2840. doi: 10.1007/s10518-015-9755-9
- Fasan M (2017) Advanced seismological and engineering analysis for structural seismic design. University of Trieste
- Fasan M (2020) Relate macroseismic intensity (EMS-98) to ground-motion parameters. SIGMA2 project report
- Fasan M, Barnaba M (2021) Database of damage-consistent natural & synthetic seismograms. SIGMA2 project report

- FEMA (2018) Seismic Performance Assessment of Buildings, FEMA P-58-1. Washington, D.C.
- Galanis PH, Moehle JP (2015) Development of Collapse Indicators for Risk Assessment of Older-Type Reinforced Concrete Buildings. *Earthquake Spectra* 31:1991–2006. doi: 10.1193/080613EQS225M
- Gehl P, Douglas J, Seyedi DM (2015) Influence of the number of dynamic analyses on the accuracy of structural response estimates. *Earthquake Spectra* 31:97–113. doi: 10.1193/102912EQS320M
- Gehl P, Seyedi DM, Douglas J (2013) Vector-valued fragility functions for seismic risk evaluation. *Bulletin of Earthquake Engineering* 11:365–384. doi: 10.1007/s10518-012-9402-7
- Grünthal G (1998) European Macroseismic Scale 1998
- Hancock J, Bommer JJ, Stafford PJ (2008) Numbers of scaled and matched accelerograms required for inelastic dynamic analyses. *Earthquake Engineering & Structural Dynamics* 37:1585–1607. doi: 10.1002/eqe.827
- Hassan HM, Fasan M, Sayed MA, et al (2020) Site-specific ground motion modeling for a historical Cairo site as a step towards computation of seismic input at cultural heritage sites. *Engineering Geology* 268:105524. doi: 10.1016/j.enggeo.2020.105524
- Iervolino I (2017) Assessing uncertainty in estimation of seismic response for PBEE. *Earthquake Engineering & Structural Dynamics* 46:1711–1723. doi: 10.1002/eqe.2883
- Jalayer F, Cornell CA (2009) Alternative non-linear demand estimation methods for probability-based seismic assessments. *Earthquake Engineering & Structural Dynamics* 38:951–972. doi: 10.1002/eqe.876
- Jalayer F, De Risi R, Manfredi G (2015) Bayesian Cloud Analysis: efficient structural fragility assessment using linear regression. *Bulletin of Earthquake Engineering* 13:1183–1203. doi: 10.1007/s10518-014-9692-z
- Jalayer F, Ebrahimian H, Miano A, et al (2017) Analytical fragility assessment using unscaled ground motion records. *Earthquake Engineering and Structural Dynamics* 46:2639–2663. doi: 10.1002/eqe.2922
- Jalayer F, Ebrahimian H, Miano A (2021) Record-to-record variability and code-compatible seismic safety-checking with limited number of records. Springer Netherlands
- Kazantzi AK, Vamvatsikos D (2015) Intensity measure selection for vulnerability studies of building classes. *Earthquake Engineering & Structural Dynamics* 44:2677–2694. doi: 10.1002/eqe.2603
- Kiani J, Camp C, Pezeshk S (2018) On the number of required response history analyses. *Bulletin of Earthquake Engineering* 16:5195–5226. doi: 10.1007/s10518-018-0381-1
- Klügel J-U, Stäuble-Akçay S (2018) Towards damage-consistent performance-based design of critical infrastructures. *International Journal of Computational Methods and Experimental Measurements* 6:933–943. doi: 10.2495/CMEM-V6-N5-933-943
- Kohrangi M, Bazzurro P, Vamvatsikos D (2016a) Vector and Scalar IMs in Structural Response Estimation, Part I: Hazard Analysis. *Earthquake Spectra* 32:1507–1524. doi: 10.1193/053115EQS080M
- Kohrangi M, Bazzurro P, Vamvatsikos D (2016b) Vector and Scalar IMs in Structural Response Estimation, Part II: Building Demand Assessment. *Earthquake Spectra* 32:1525–1543. doi: 10.1193/053115EQS081M
- Kohrangi M, Vamvatsikos D, Bazzurro P (2016c) Implications of intensity measure selection for seismic loss assessment of 3-D buildings. *Earthquake Spectra* 32:2167–2189. doi: 10.1193/112215EQS177M
- Kohrangi M, Vamvatsikos D, Bazzurro P (2017) Site dependence and record selection schemes for building fragility and regional loss assessment. *Earthquake Engineering and Structural Dynamics* 46:1625–1643. doi: 10.1002/eqe.2873
- Luco N, Bazzurro P (2007) Does amplitude scaling of ground motion records result in biased nonlinear structural drift responses? *Earthquake Engineering & Structural Dynamics* 36:1813–1835. doi: 10.1002/eqe.2873
- M. Fasan - Develop fragility curves as a function of intensity for full SRA in Intensity domain –  
SIGMA2\_2021\_D6\_087

10.1002/eqe.695

- Luco N, Cornell CA (2007) Structure-specific scalar intensity measures for near-source and ordinary earthquake ground motions. *Earthquake Spectra* 23:357–392. doi: 10.1193/1.2723158
- Mander JB, Priestley MJN, Park R (1988) Theoretical Stress-Strain Model for Confined Concrete. *Journal of Structural Engineering* 114:1804–1826. doi: 10.1061/(ASCE)0733-9445(1988)114:8(1804)
- Modica A, Stafford PJ (2014) Vector fragility surfaces for reinforced concrete frames in Europe. *Bulletin of Earthquake Engineering* 12:1725–1753. doi: 10.1007/s10518-013-9571-z
- Musson RMW, Grünthal G, Stucchi M (2010) The comparison of macroseismic intensity scales. *Journal of Seismology* 14:413–428. doi: 10.1007/s10950-009-9172-0
- Padgett JE, Nielson BG, DesRoches R (2008) Selection of optimal intensity measures in probabilistic seismic demand models of highway bridge portfolios. *Earthquake Engineering & Structural Dynamics* 37:711–725. doi: 10.1002/eqe.782
- Paolucci R, Gatti F, Infantino M, et al (2018) Broadband Ground Motions from 3D Physics-Based Numerical Simulations Using Artificial Neural Networks. *Bulletin of the Seismological Society of America* 108:1272–1286. doi: 10.1785/0120170293
- Pitilakis K, Crowley H, Kaynia AM (eds) (2014) SYNER-G: Typology Definition and Fragility Functions for Physical Elements at Seismic Risk. Springer Netherlands, Dordrecht
- Reed JW, Kassawara RP (1990) A criterion for determining exceedance of the operating basis earthquake. *Nuclear Engineering and Design* 123:387–396. doi: 10.1016/0029-5493(90)90259-Z
- Seismosoft (2021) SeismoStruct 2021 – A computer program for static and dynamic nonlinear analysis of framed structures
- Shome N, Cornell (1999) Probabilistic Seismic Demand Analysis of Nonlinear Structures. Stanford, CA
- Silva V, Akkar S, Baker J, et al (2019) Current challenges and future trends in analytical fragility and vulnerability modeling. *Earthquake Spectra* 35:1927–1952. doi: 10.1193/042418EQS1010
- Vamvatsikos D, Cornell CA (2002) Incremental dynamic analysis. *Earthquake Engineering and Structural Dynamics* 31:491–514. doi: 10.1002/eqe.141
- Zacharenaki A, Fragiadakis M, Assimaki D, Papadrakakis M (2014) Bias assessment in Incremental Dynamic Analysis due to record scaling. *Soil Dynamics and Earthquake Engineering* 67:158–168. doi: 10.1016/j.soildyn.2014.09.007

## APPENDIX 1 Estimated median fragility parameters

**Table 4: Parameters of the estimated fragility for MIDR**

$IM$	$a^{50th}$	$b^{50th}$	$\sigma_{\ln(MIDR) \ln(IM)}^{50th}$	$\alpha_0^{50th}$	$\alpha_1^{50th}$
$PGA_{GM}$	-3.482	0.852	0.375	-1.769	3.231
$PGA_{RotD50}$	-3.554	0.830	0.379	-2.048	3.126
$PGA_{RotD100}$	-3.768	0.819	0.385	-2.777	2.975
$PGA_{GMRotD50}$	-3.500	0.843	0.369	-1.870	3.196
$PGA_{GMRotD100}$	-3.568	0.836	0.374	-2.118	3.149
$CAV_{GM}$	-5.829	0.771	0.432	-9.675	2.698
$CAV_{RotD50}$	-5.865	0.767	0.429	-9.663	2.635
$CAV_{RotD100}$	-6.000	0.760	0.441	-9.809	2.535
$CAV_{GMRotD50}$	-5.828	0.768	0.425	-9.632	2.657
$CAV_{GMRotD100}$	-5.869	0.769	0.428	-9.676	2.640
$PSA_{GM}$	-3.416	0.854	0.308	-1.801	3.366
$PSA_{RotD50}$	-3.440	0.841	0.300	-1.956	3.373
$PSA_{RotD100}$	-3.507	0.836	0.304	-2.223	3.365
$PSA_{GMRotD50}$	-3.495	0.835	0.307	-2.163	3.339
$PSA_{GMRotD100}$	-3.713	0.815	0.325	-2.949	3.244
$PSA_{avg,GM}$	-3.402	0.953	0.224	-2.207	4.053
$PSA_{avg,RotD50}$	-3.428	0.939	0.216	-2.382	4.164
$PSA_{avg,RotD100}$	-3.498	0.938	0.216	-2.712	4.156
$PSA_{avg,GMRotD50}$	-3.479	0.938	0.215	-2.617	4.136
$PSA_{avg,GMRotD100}$	-3.716	0.930	0.220	-3.515	3.939
$I_{EMS,avg}$	-14.013	5.028	0.392	-38.925	17.793
$I_{EMS}$	-8.642	2.243	0.683	-9.213	3.633

**Table 5: Parameters of the estimated fragility for PFA**

$IM$	$a^{50th}$	$b^{50th}$	$\sigma_{\ln(PFA) \ln(IM)}^{50th}$	$\alpha_0^{50th}$	$\alpha_1^{50th}$
$PGA_{GM}$	2.396	0.772	0.160	-1.769	3.231
$PGA_{RotD50}$	2.336	0.760	0.138	-2.048	3.126
$PGA_{RotD100}$	2.142	0.754	0.130	-2.777	2.975
$PGA_{GMRotD50}$	2.379	0.764	0.147	-1.870	3.196
$PGA_{GMRotD100}$	2.320	0.762	0.141	-2.118	3.149
$CAV_{GM}$	0.343	0.665	0.317	-9.675	2.698
$CAV_{RotD50}$	0.304	0.666	0.307	-9.663	2.635
$CAV_{RotD100}$	0.165	0.668	0.304	-9.809	2.535
$CAV_{GMRotD50}$	0.344	0.662	0.309	-9.632	2.657
$CAV_{GMRotD100}$	0.301	0.667	0.305	-9.676	2.640
$PSA_{GM}$	2.374	0.671	0.324	-1.801	3.366
$PSA_{RotD50}$	2.355	0.661	0.318	-1.956	3.373
$PSA_{RotD100}$	2.303	0.659	0.317	-2.223	3.365
$PSA_{GMRotD50}$	2.313	0.659	0.317	-2.163	3.339
$PSA_{GMRotD100}$	2.143	0.648	0.319	-2.949	3.244
$PSA_{avg,GM}$	2.391	0.758	0.256	-2.207	4.053
$PSA_{avg,RotD50}$	2.372	0.749	0.249	-2.382	4.164
$PSA_{avg,RotD100}$	2.316	0.750	0.245	-2.712	4.156
$PSA_{avg,GMRotD50}$	2.332	0.751	0.244	-2.617	4.136
$PSA_{avg,GMRotD100}$	2.144	0.748	0.239	-3.515	3.939
$I_{EMS,avg}$	-6.866	4.414	0.249	-38.925	17.793
$I_{EMS}$	-2.240	2.013	0.546	-9.213	3.633

## APPENDIX 2 Efficiency and proficiency for the different PLs

**Table 6: Efficiency  $\sigma_{\ln(EDP)|\ln(IM)}$  and proficiency  $\sigma_{\ln(IM)|\ln(EDP)}$  for the five considered PLs - MIDR**

<i>IM</i>	$\sigma_{\ln(EDP) \ln(IM)}$	$\sigma_{\ln(IM_{IO}) \ln(EDP)}$	$\sigma_{\ln(IM_{DL}) \ln(EDP)}$	$\sigma_{\ln(IM_{LS}) \ln(EDP)}$	$\sigma_{\ln(IM_{CP}) \ln(EDP)}$	$\sigma_{\ln(IM_C) \ln(EDP)}$
<i>PGA<sub>GM</sub></i>	0.375	0.438	0.437	0.407	0.407	0.427
<i>PGA<sub>RotD50</sub></i>	0.379	0.455	0.454	0.422	0.422	0.440
<i>PGA<sub>RotD100</sub></i>	0.385	0.467	0.467	0.435	0.435	0.458
<i>PGA<sub>GMRotD50</sub></i>	0.369	0.435	0.435	0.406	0.406	0.429
<i>PGA<sub>GMRotD100</sub></i>	0.374	0.444	0.444	0.414	0.414	0.436
<i>CAV<sub>GM</sub></i>	0.432	0.557	0.555	0.505	0.505	0.518
<i>CAV<sub>RotD50</sub></i>	0.429	0.555	0.553	0.507	0.507	0.525
<i>CAV<sub>RotD100</sub></i>	0.441	0.577	0.575	0.525	0.525	0.546
<i>CAV<sub>GMRotD50</sub></i>	0.425	0.550	0.548	0.503	0.503	0.521
<i>CAV<sub>GMRotD100</sub></i>	0.428	0.552	0.551	0.505	0.505	0.524
<i>PSA<sub>GM</sub></i>	0.308	0.358	0.358	0.345	0.345	0.396
<i>PSA<sub>RotD50</sub></i>	0.300	0.354	0.354	0.342	0.342	0.395
<i>PSA<sub>RotD100</sub></i>	0.304	0.361	0.361	0.347	0.347	0.397
<i>PSA<sub>GMRotD50</sub></i>	0.307	0.365	0.365	0.352	0.352	0.399
<i>PSA<sub>GMRotD100</sub></i>	0.325	0.396	0.396	0.377	0.377	0.416
<i>PSA<sub>avg,GM</sub></i>	0.224	0.234	0.234	0.232	0.232	0.313
<i>PSA<sub>avg,RotD50</sub></i>	0.216	0.228	0.229	0.227	0.227	0.309
<i>PSA<sub>avg,RotD100</sub></i>	0.216	0.228	0.229	0.227	0.227	0.308
<i>PSA<sub>avg,GMRotD50</sub></i>	0.215	0.228	0.228	0.227	0.227	0.309
<i>PSA<sub>avg,GMRotD100</sub></i>	0.220	0.235	0.235	0.234	0.234	0.322
<i>I<sub>EMS,avg</sub></i>	0.392	0.078	0.077	0.072	0.072	0.077
<i>I<sub>EMS</sub></i>	0.683	0.299	0.297	0.296	0.296	0.330

**Table 7: Efficiency  $\sigma_{\ln(EDP)|\ln(IM)}$  and proficiency  $\sigma_{\ln(IM)|\ln(EDP)}$  for the five considered PLs - PFA**

<i>IM</i>	$\sigma_{\ln(EDP) \ln(IM)}$	$\sigma_{\ln(IM_{IO}) \ln(EDP)}$	$\sigma_{\ln(IM_{DL}) \ln(EDP)}$	$\sigma_{\ln(IM_{LS}) \ln(EDP)}$	$\sigma_{\ln(IM_{CP}) \ln(EDP)}$	$\sigma_{\ln(IM_C) \ln(EDP)}$
<i>PGA<sub>GM</sub></i>	0.160	0.207	0.207	0.207	0.207	0.257
<i>PGA<sub>RotD50</sub></i>	0.138	0.181	0.181	0.182	0.182	0.242
<i>PGA<sub>RotD100</sub></i>	0.130	0.172	0.173	0.174	0.174	0.241
<i>PGA<sub>GMRotD50</sub></i>	0.147	0.191	0.191	0.192	0.192	0.247
<i>PGA<sub>GMRotD100</sub></i>	0.141	0.185	0.185	0.186	0.186	0.244
<i>CAV<sub>GM</sub></i>	0.317	0.471	0.469	0.465	0.465	0.447
<i>CAV<sub>RotD50</sub></i>	0.307	0.456	0.454	0.451	0.451	0.443
<i>CAV<sub>RotD100</sub></i>	0.304	0.451	0.449	0.447	0.447	0.449
<i>CAV<sub>GMRotD50</sub></i>	0.309	0.463	0.461	0.458	0.458	0.445
<i>CAV<sub>GMRotD100</sub></i>	0.305	0.453	0.452	0.449	0.449	0.441
<i>PSA<sub>GM</sub></i>	0.324	0.479	0.477	0.473	0.473	0.406
<i>PSA<sub>RotD50</sub></i>	0.318	0.477	0.475	0.472	0.472	0.405
<i>PSA<sub>RotD100</sub></i>	0.317	0.478	0.476	0.473	0.473	0.406
<i>PSA<sub>GMRotD50</sub></i>	0.317	0.478	0.476	0.472	0.472	0.407
<i>PSA<sub>GMRotD100</sub></i>	0.319	0.489	0.487	0.483	0.483	0.417
<i>PSA<sub>avg,GM</sub></i>	0.256	0.336	0.335	0.334	0.334	0.306
<i>PSA<sub>avg,RotD50</sub></i>	0.249	0.330	0.330	0.329	0.329	0.300
<i>PSA<sub>avg,RotD100</sub></i>	0.245	0.325	0.324	0.323	0.323	0.297
<i>PSA<sub>avg,GMRotD50</sub></i>	0.244	0.323	0.322	0.321	0.321	0.296
<i>PSA<sub>avg,GMRotD100</sub></i>	0.239	0.318	0.317	0.317	0.317	0.299
<i>I<sub>EMS,avg</sub></i>	0.249	0.056	0.056	0.056	0.056	0.059
<i>I<sub>EMS</sub></i>	0.546	0.267	0.267	0.267	0.267	0.287

### APPENDIX 3 Sufficiency parameters value

**Table 8: Estimated slope  $b$ , standard deviation  $\sigma$ ,  $p$  – value and  $R^2$  for Mw - MIDR**

$IM$	$b$	$\sigma$	$p$ – value	$R^2$
$PGA_{GM}$	0.502	0.678	1.76E-10	0.128
$PGA_{RotD50}$	0.486	0.679	6.12E-10	0.121
$PGA_{RotD100}$	0.489	0.676	4.37E-10	0.123
$PGA_{GMRotD50}$	0.499	0.682	2.90E-10	0.125
$PGA_{GMRotD100}$	0.490	0.681	5.43E-10	0.121
$CAV_{GM}$	0.876	0.525	7.03E-38	0.427
$CAV_{RotD50}$	0.871	0.529	3.82E-37	0.420
$CAV_{RotD100}$	0.845	0.531	2.09E-35	0.404
$CAV_{GMRotD50}$	0.882	0.529	7.65E-38	0.426
$CAV_{GMRotD100}$	0.871	0.531	5.06E-37	0.419
$PSA_{GM}$	0.649	0.679	7.22E-16	0.196
$PSA_{RotD50}$	0.656	0.681	4.62E-16	0.199
$PSA_{RotD100}$	0.650	0.681	7.94E-16	0.196
$PSA_{GMRotD50}$	0.641	0.682	1.90E-15	0.191
$PSA_{GMRotD100}$	0.629	0.676	3.46E-15	0.188
$PSA_{avg,GM}$	0.695	0.701	7.60E-17	0.208
$PSA_{avg,RotD50}$	0.690	0.704	1.63E-16	0.204
$PSA_{avg,RotD100}$	0.684	0.706	3.15E-16	0.201
$PSA_{avg,GMRotD50}$	0.677	0.708	7.16E-16	0.196
$PSA_{avg,GMRotD100}$	0.667	0.709	1.86E-15	0.191
$I_{EMS,avg}$	0.575	0.653	6.50E-14	0.172
$I_{EMS}$	0.234	0.428	1.71E-06	0.074



**Table 9: Estimated slope  $b$ , standard deviation  $\sigma$ ,  $p$  – value and  $R^2$  for Repi - MIDR**

$IM$	$b$	$\sigma$	$p$ – value	$R^2$
$PGA_{GM}$	-0.411	0.671	6.54E-12	0.147
$PGA_{RotD50}$	-0.400	0.672	2.19E-11	0.140
$PGA_{RotD100}$	-0.386	0.673	1.05E-10	0.131
$PGA_{GMRotD50}$	-0.410	0.675	9.49E-12	0.144
$PGA_{GMRotD100}$	-0.404	0.674	1.67E-11	0.141
$CAV_{GM}$	-0.164	0.685	5.46E-03	0.026
$CAV_{RotD50}$	-0.157	0.687	8.22E-03	0.023
$CAV_{RotD100}$	-0.137	0.681	1.92E-02	0.018
$CAV_{GMRotD50}$	-0.167	0.689	5.09E-03	0.026
$CAV_{GMRotD100}$	-0.158	0.688	7.81E-03	0.024
$PSA_{GM}$	-0.297	0.731	3.09E-06	0.071
$PSA_{RotD50}$	-0.305	0.733	1.94E-06	0.073
$PSA_{RotD100}$	-0.303	0.731	2.06E-06	0.073
$PSA_{GMRotD50}$	-0.302	0.730	2.13E-06	0.073
$PSA_{GMRotD100}$	-0.294	0.724	3.24E-06	0.070
$PSA_{avg,GM}$	-0.341	0.753	2.44E-07	0.086
$PSA_{avg,RotD50}$	-0.341	0.755	2.65E-07	0.085
$PSA_{avg,RotD100}$	-0.338	0.756	3.45E-07	0.084
$PSA_{avg,GMRotD50}$	-0.336	0.757	3.89E-07	0.083
$PSA_{avg,GMRotD100}$	-0.330	0.756	5.94E-07	0.080
$I_{EMS,avg}$	-0.278	0.692	4.21E-06	0.069
$I_{EMS}$	-0.115	0.438	2.36E-03	0.031

**Table 10: Estimated slope  $b$ , standard deviation  $\sigma$ ,  $p$  – value and  $R^2$  for Vs,30 - MIDR**

$IM$	$b$	$\sigma$	$p$ – value	$R^2$
$PGA_{GM}$	-0.535	0.657	1.38E-14	0.181
$PGA_{RotD50}$	-0.521	0.659	7.02E-14	0.172
$PGA_{RotD100}$	-0.517	0.658	9.03E-14	0.170
$PGA_{GMRotD50}$	-0.532	0.662	2.82E-14	0.177
$PGA_{GMRotD100}$	-0.531	0.659	2.60E-14	0.177
$CAV_{GM}$	-0.647	0.585	7.50E-24	0.289
$CAV_{RotD50}$	-0.641	0.589	2.78E-23	0.283
$CAV_{RotD100}$	-0.634	0.582	3.02E-23	0.282
$CAV_{GMRotD50}$	-0.641	0.593	4.74E-23	0.280
$CAV_{GMRotD100}$	-0.642	0.590	2.60E-23	0.283
$PSA_{GM}$	-0.588	0.678	3.70E-16	0.200
$PSA_{RotD50}$	-0.582	0.683	1.07E-15	0.194
$PSA_{RotD100}$	-0.576	0.683	1.89E-15	0.191
$PSA_{GMRotD50}$	-0.574	0.682	2.30E-15	0.190
$PSA_{GMRotD100}$	-0.554	0.679	1.25E-14	0.181
$PSA_{avg,GM}$	-0.616	0.703	1.98E-16	0.203
$PSA_{avg,RotD50}$	-0.616	0.705	2.55E-16	0.202
$PSA_{avg,RotD100}$	-0.616	0.705	2.39E-16	0.202
$PSA_{avg,GMRotD50}$	-0.616	0.706	2.69E-16	0.202
$PSA_{avg,GMRotD100}$	-0.612	0.705	3.47E-16	0.200
$I_{EMS,avg}$	-0.542	0.646	2.54E-15	0.190
$I_{EMS}$	-0.201	0.430	4.66E-06	0.068

**Table 11: Estimated slope  $b$ , standard deviation  $\sigma$ ,  $p$  – value and  $R^2$  for Mw - PFA**

$IM$	$b$	$\sigma$	$p$ – value	$R^2$
$PGA_{GM}$	0.455	0.614	1.76E-10	0.128
$PGA_{RotD50}$	0.445	0.622	6.12E-10	0.121
$PGA_{RotD100}$	0.450	0.623	4.37E-10	0.123
$PGA_{GMRotD50}$	0.452	0.618	2.90E-10	0.125
$PGA_{GMRotD100}$	0.446	0.621	5.43E-10	0.121
$CAV_{GM}$	0.756	0.453	7.03E-38	0.427
$CAV_{RotD50}$	0.756	0.460	3.82E-37	0.420
$CAV_{RotD100}$	0.744	0.467	2.09E-35	0.404
$CAV_{GMRotD50}$	0.760	0.456	7.65E-38	0.426
$CAV_{GMRotD100}$	0.756	0.460	5.06E-37	0.419
$PSA_{GM}$	0.510	0.534	7.22E-16	0.196
$PSA_{RotD50}$	0.516	0.535	4.62E-16	0.199
$PSA_{RotD100}$	0.512	0.536	7.94E-16	0.196
$PSA_{GMRotD50}$	0.506	0.538	1.90E-15	0.191
$PSA_{GMRotD100}$	0.500	0.538	3.46E-15	0.188
$PSA_{avg,GM}$	0.553	0.558	7.60E-17	0.208
$PSA_{avg,RotD50}$	0.550	0.562	1.63E-16	0.204
$PSA_{avg,RotD100}$	0.547	0.564	3.15E-16	0.201
$PSA_{avg,GMRotD50}$	0.542	0.567	7.16E-16	0.196
$PSA_{avg,GMRotD100}$	0.536	0.570	1.86E-15	0.191
$I_{EMS,avg}$	0.505	0.573	6.50E-14	0.172
$I_{EMS}$	0.210	0.384	1.71E-06	0.074

**Table 12: Estimated slope  $b$ , standard deviation  $\sigma$ ,  $p$  – value and  $R^2$  for Rept - PFA**

$IM$	$b$	$\sigma$	$p$ – value	$R^2$
$PGA_{GM}$	-0.372	0.608	6.54E-12	0.147
$PGA_{RotD50}$	-0.366	0.615	2.19E-11	0.140
$PGA_{RotD100}$	-0.355	0.620	1.05E-10	0.131
$PGA_{GMRotD50}$	-0.371	0.612	9.49E-12	0.144
$PGA_{GMRotD100}$	-0.368	0.614	1.67E-11	0.141
$CAV_{GM}$	-0.142	0.591	5.46E-03	0.026
$CAV_{RotD50}$	-0.136	0.597	8.22E-03	0.023
$CAV_{RotD100}$	-0.121	0.599	1.92E-02	0.018
$CAV_{GMRotD50}$	-0.144	0.594	5.09E-03	0.026
$CAV_{GMRotD100}$	-0.137	0.597	7.81E-03	0.024
$PSA_{GM}$	-0.234	0.574	3.09E-06	0.071
$PSA_{RotD50}$	-0.239	0.576	1.94E-06	0.073
$PSA_{RotD100}$	-0.239	0.576	2.06E-06	0.073
$PSA_{GMRotD50}$	-0.238	0.576	2.13E-06	0.073
$PSA_{GMRotD100}$	-0.234	0.576	3.24E-06	0.070
$PSA_{avg,GM}$	-0.271	0.600	2.44E-07	0.086
$PSA_{avg,RotD50}$	-0.272	0.602	2.65E-07	0.085
$PSA_{avg,RotD100}$	-0.270	0.604	3.45E-07	0.084
$PSA_{avg,GMRotD50}$	-0.269	0.605	3.89E-07	0.083
$PSA_{avg,GMRotD100}$	-0.266	0.608	5.94E-07	0.080
$I_{EMS,avg}$	-0.244	0.608	4.21E-06	0.069
$I_{EMS}$	-0.103	0.393	2.36E-03	0.031

**Table 13: Estimated slope  $b$ , standard deviation  $\sigma$ ,  $p$  – value and  $R^2$  for Vs,30 - PFA**

$IM$	$b$	$\sigma$	$p$ – value	$R^2$
$PGA_{GM}$	-0.485	0.596	1.38E-14	0.181
$PGA_{RotD50}$	-0.477	0.604	7.02E-14	0.172
$PGA_{RotD100}$	-0.476	0.605	9.03E-14	0.170
$PGA_{GMRotD50}$	-0.482	0.600	2.82E-14	0.177
$PGA_{GMRotD100}$	-0.484	0.601	2.60E-14	0.177
$CAV_{GM}$	-0.558	0.505	7.50E-24	0.289
$CAV_{RotD50}$	-0.557	0.511	2.78E-23	0.283
$CAV_{RotD100}$	-0.557	0.512	3.02E-23	0.282
$CAV_{GMRotD50}$	-0.553	0.511	4.74E-23	0.280
$CAV_{GMRotD100}$	-0.558	0.512	2.60E-23	0.283
$PSA_{GM}$	-0.462	0.533	3.70E-16	0.200
$PSA_{RotD50}$	-0.457	0.537	1.07E-15	0.194
$PSA_{RotD100}$	-0.454	0.538	1.89E-15	0.191
$PSA_{GMRotD50}$	-0.453	0.538	2.30E-15	0.190
$PSA_{GMRotD100}$	-0.441	0.540	1.25E-14	0.181
$PSA_{avg,GM}$	-0.490	0.560	1.98E-16	0.203
$PSA_{avg,RotD50}$	-0.491	0.563	2.55E-16	0.202
$PSA_{avg,RotD100}$	-0.493	0.564	2.39E-16	0.202
$PSA_{avg,GMRotD50}$	-0.492	0.565	2.69E-16	0.202
$PSA_{avg,GMRotD100}$	-0.492	0.567	3.47E-16	0.200
$I_{EMS,avg}$	-0.476	0.567	2.54E-15	0.190
$I_{EMS}$	-0.181	0.386	4.66E-06	0.068